

**Experimental Studies on Wave Attenuation of an  
Innovative Multipurpose Submerged Breakwater (M-Sub)**

by

Na Kai Lun

Dissertation submitted in partial fulfilment of  
the requirements for the  
Bachelor of Engineering (Hons)  
(Civil Engineering)

SEPTEMBER 2011

Universiti Teknologi PETRONAS  
Bandar Seri Iskandar  
31750 Tronoh  
Perak Darul Ridzuan

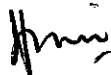
CERTIFICATION OF APPROVAL

**Experimental Studies on Wave Attenuation of an Innovative Multipurpose  
Submerged Breakwater (M-Sub)**

by  
Na Kai Lun

A project dissertation submitted to the  
Civil Engineering Programme  
Universiti Teknologi PETRONAS  
in partial fulfilment of the requirement for the  
BACHELOR OF ENGINEERING (Hons)  
(CIVIL ENGINEERING)

Approved by,



---

(Assoc. Prof. Ahmad Mustafa B. Hashim)  
Project Supervisor

UNIVERSITI TEKNOLOGI PETRONAS

TRONOH, PERAK

SEPTEMBER 2011

## CERTIFICATION OF ORIGINALITY

This is to certify that the author is responsible for the work submitted in this project, that the original work is her own except as specified in the references and acknowledgements, and that the original work contained herein have not been undertaken or done by unspecified sources or persons.

---

NA KAI LUN

## ABSTRACT

Submerged breakwaters have been widely used for the protection of coastal habitats. However, as with the many designs in the market, there have been mixed reviews on the current array of submerged breakwaters. Hence, there is definitely room for innovations. A multipurpose submerged breakwater (M-Sub) is designed staggered to study the wave transmission effects of its corresponding vortices and turbulence. In its conceptual stage, it is suitable for areas of moderate/low wave energy climate. Besides being a possible solution to coastal erosion, it holds potential as a fish habitat enhancer. This study is designed to investigate the transmissive abilities (in terms of transmission coefficient,  $K_t$ ) of this innovative breakwater shape. The objective is to obtain experimental data and wave attenuating abilities of the model subjected to regular and random waves in an array of wave parameters and structure porosity. Results from the 144 tests conducted revealed good resemblance with the expected trend calculated using d'Angremond. The M-Sub worked best for the wave height of 0.18 m and wave period of 1.12 s, whereas its porous version was found to return a lower  $K_t$  value when tested with 0.16 m waves. Nevertheless, additional experiments should be conducted to enhance the initial findings by including more variables such as wave variability and structure configurations.

## **ACKNOWLEDGEMENT**

The author would like to thank Assoc. Prof. Ahmad Mustafa Hashim for his direction, as well as guidance throughout the 8-month-course of this study.

A special thank-you also goes out to the Civil Engineering Department of Universiti Teknologi PETRONAS, particularly technicians Mr Meor, Mr Idris, Mr Hafiz and Mr Johan for their assistance, contributions of valuable technical knowledge and kind cooperation during the course the author's laboratory stints.

Last but not least, a great deal of appreciation is expressed towards friends and family for their moral support.

## TABLE OF CONTENTS

|   |      |
|---|------|
| CERTIFICATION .....   | ii   |
| ABSTRACT .....  | iv   |
| ACKNOWLEDGMENT .....  | v    |
| LIST OF FIGURES .....   | viii |
| LIST OF TABLES .....  | x    |
| CHAPTER 1 .....   | 1    |
| INTRODUCTION .....  | 1    |
| 1.1 Background of Study.....                                  | 1    |
| 1.2 Problem Statement .....                                   | 3    |
| 1.3 Objectives and Scope of Study.....                        | 3    |
| 1.4 Relevancy of Study .....                                  | 4    |
| CHAPTER 2 .....   | 5    |
| LITERATURE REVIEW .....                                       | 5    |
| 2.1 Wave Mechanics .....                                      | 5    |
| 2.2 Characteristics of a Nearshore Submerged Breakwater ..... | 6    |
| 2.2.1. Transmission Characteristics .....                     | 7    |
| 2.2.2. Porosity .....   | 11   |
| 2.3. Characteristics of a Fish Habitat Enhancer .....         | 12   |
| CHAPTER 3 .....   | 15   |
| METHODOLOGY .....   | 15   |
| 3.1 Project Activities .....                                  | 15   |
| 3.2 Equipment and Tools .....                                 | 17   |
| 3.4 Key Milestones and Gantt Chart .....                      | 20   |

|  |    |
|--|----|
| CHAPTER 4 .....                                      | 21 |
| RESULTS AND DISCUSSION .....                         | 21 |
| 4.1 Results for 0.70 m water depth.....              | 22 |
| 4.2 Results for 0.65 m water depth.....              | 30 |
| 4.3 Results for 0.60m water depth.....               | 37 |
| CHAPTER 5 .....                                      | 44 |
| CONCLUSION AND RECOMMENDATIONS .....                 | 44 |
| 5.1 Relevancy to the Objectives .....                | 44 |
| REFERENCES .....                                     | 46 |
| APPENDIX A: WAVE CHARACTERISTICS OF EAST COAST ..... | 50 |
| APPENDIX B: MISCELLANEOUS.....                       | 52 |

## LIST OF FIGURES

|   |    |
|---|----|
| Figure 1: Wave mechanics and important connotations of a submerged<br>breakwater .....                        | 5  |
| Figure 2: Graph of $K_t$ as a function of $R_o/H_i$ for given values of $B/L$ . .....                         | 9  |
| Figure 3: Graph of $K_t$ as a function of $B/L$ for given values of $R_o/H_i$ . .....                         | 9  |
| Figure 4: Graphs of $d_f/H_i$ in relation to $C_o$ , $C_r$ and $C_d$ . Source: Bleck, 2006 .....              | 10 |
| Figure 5: Methodology and general flow of the study .....   | 16 |
| Figure 6: Experimental settings. A, B, C, D and E denotes the location of wave<br>gauges .....                | 16 |
| Figure 7: (Above) Side view and (Below) Plan view of the wave flume used for<br>this study .....              | 18 |
| Figure 8: Different units of the two types of model breakwater .....  | 19 |
| Figure 9: Configuration of the breakwater mode .....  | 19 |
| Figure 10: Gantt Chart and Key Milestones for FYP 1 and FYP2 .....  | 20 |
| Figure 11: $K_t$ as a function of $B/L$ , given $R_o/H_i$ for regular wave conditions .....                   | 24 |
| Figure 12: $K_t$ as a function of $B/L$ , given $R_o/H_i$ for random wave conditions .....                    | 25 |
| Figure 13: $K_t$ as a function of $R_o/H_i$ given $B/L$ for regular wave conditions<br>( $d=0.70m$ ) .....    | 27 |
| Figure 14: $K_t$ as a function of $R_o/H_i$ given $B/L$ for random wave conditions .....                      | 27 |
| Figure 15: Comparison of calculated and measured $K_t$ for regular wave<br>conditions ( $d=0.70 m$ ) .....    | 28 |
| Figure 16: Comparison of calculated and measured $K_t$ for random wave<br>conditions ( $d=0.70 m$ ) .....     | 29 |
| Figure 17: $K_t$ as a function of $B/L$ , given $R_o/H_i$ for regular wave conditions<br>( $d=0.65 m$ ) ..... | 32 |
| Figure 18: $K_t$ as a function of $B/L$ , given $R_o/H_i$ for random waves at ( $d=0.65 m$ ) .....            | 33 |
| Figure 19: $K_t$ as a function of $R_o/H_i$ given $B/L$ for regular wave conditions<br>( $d=0.65 m$ ) .....   | 34 |

|  |    |
|--|----|
| Figure 20: $K_t$ as a function of $R_o/H_i$ given $B/L$ for random wave conditions<br>( $d=0.65$ m) .....    | 35 |
| Figure 21: Comparison of calculated and measured $K_t$ for regular wave<br>conditions ( $d=0.65$ m) .....    | 35 |
| Figure 22: Comparison of calculated and measured $K_t$ for random wave<br>conditions ( $d=0.65$ m) .....     | 36 |
| Figure 23: $K_t$ as a function of $B/L$ , given $R_o/H_i$ for regular wave conditions<br>( $d=0.60$ m) ..... | 39 |
| Figure 24: $K_t$ as a function of $B/L$ , given $R_o/H_i$ for random wave conditions<br>( $d=0.60$ m) .....  | 40 |
| Figure 25: $K_t$ as a function of $R_o/H_i$ given $B/L$ for regular wave conditions.....                     | 41 |
| Figure 26: $K_t$ as a function of $R_o/H_i$ given $B/L$ for random wave conditions<br>( $d=0.60$ m) .....    | 42 |
| Figure 27: Comparison of calculated and measured $K_t$ for regular wave<br>conditions ( $d=0.60$ m) .....    | 42 |
| Figure 28: Comparison of calculated and measured $K_t$ for random wave<br>conditions ( $d=0.60$ m) .....     | 43 |

## LIST OF TABLES

|  |    |
|--|----|
| Table 1 : Dimensions of individual test model unit.....  | 11 |
| Table 2: Comparison of results between two porosity studies.....   | 12 |
| Table 3: Wave characteristics employed in the study.....   | 17 |
| Table 4: Summary of wave parameters and their corresponding transmission<br>coefficient at water depth of 0.70 m.....  | 22 |
| Table 5: Experimental results for non-porous model ( $K_t$ 1) at water depth 0.70<br>m.....                            | 23 |
| Table 6: Experimental results for porous model ( $K_t$ 2) at water depth 0.70m.....                                    | 23 |
| Table 7: Summary of wave parameters and their corresponding transmission<br>coefficient at water depth of 0.65 m.....  | 30 |
| Table 8: Experimental results for non-porous model ( $K_t$ 1) at water depth 0.65<br>m.....                            | 31 |
| Table 9: Experimental results for porous model ( $K_t$ 2) at water depth 0.65 m.....                                   | 31 |
| Table 10: Summary of wave parameters and their corresponding transmission<br>coefficient at water depth of 0.60 m..... | 37 |
| Table 11: Experimental results for non-porous model ( $K_t$ 1) at water depth 0.60<br>m.....                           | 38 |
| Table 12: Experimental results for non-porous model ( $K_t$ 2) at water depth<br>0.60m.....                            | 38 |

## CHAPTER 1

### INTRODUCTION

#### 1.1 Background of Study

Encapsulating almost 70 % of Malaysian land, coastal zones are the centre of a lot of economic happenings; such as urbanization, industrial activities, shipping, recreation and tourism and aquaculture. Also, nearshore habitats of estuaries support an extensive spectrum of marine life and serve as nursery grounds for economically-important fishes and shellfish (Beck et al., 2001) (Coen et al., 1999) (Heck, 2003).

Demands and developments of these areas naturally caused gradual changes which potentially lead to erosion to the coastline. Erosion is identified as a national problem with more than 29 % or 1380 km of Malaysia coastline facing erosion (DID, 2011). Among the more affected are the coastlines bordering the South China Sea.

The most important cause of human-induced erosion is the interruption of sediment sources and longshore sediment transport (U.S. Army Corps of Engineers, 1984). Examples include the mining of sediment source and the interruption of longshore sediment transport by the construction of groins and jetties. Increasing wave energy along the coastlines is also found to be damaging. This surge is tied back to global warming, increased boat activities, and excessive implementation of manmade structures (Church, 2007).

Conventionally, hard structural measures such as bulkheads and seawalls were implemented to remedy erosion. However, there are a growing number of discussions refuting the efficiency of these structures; in terms of ecology-friendliness (Swann, 2008). Therefore, alternatives such as living shorelines, which stabilizes the coastline as well as protect surrounding intertidal environment and habitat, are gaining a reputation.

One good example is breakwater. Its main principles are to reduce the amount of wave energy in their lee, and to initiate sediment deposition at the shoreline through the modification of waves (Pilarczyk, 2003). Additionally, as breakwaters are typically not of continuous length along the shoreline, the gaps provide an escape to aquatic life that would become trapped during ebb tide as well as continuous flow of water.

Submerged breakwaters are perceived to be capable of providing the necessary beach protection without any negative effects such as reflection of waves and aesthetics issues posed by emergent structures. The use of such submerged breakwaters in the surf zone also provides optimization of bathymetry to enhance local surfing and swimming conditions (Ranasinghe et al., 2001) as only larger waves are attenuated while smaller waves are transmitted (Dally and Pope, 1986). Lastly, the cost of constructing a submerged breakwater would be cheaper as compared that of an emergent one. Thus, submerged breakwaters are much feasible means in overcoming complications of emergent breakwaters.

An innovative multipurpose submerged breakwater (M-Sub) designed with a unique arrangement is investigated on its performance in dissipating wave energy (in terms of transmission coefficient,  $K_t$ ) through enhanced turbulence and vortices. Conceptually, it is suitable for areas of moderate/low wave energy climate. Besides being a possible solution to coastal erosion, it holds potential as a fish habitat enhancer.

## **1.2 Problem Statement**

Coastlines have always played a significant part in the development and tourism of a country. With the increase in the frequency and the strength of storm surges observed in the last decades, effective shoreline protection would ensure the safety of residents and tourists alike.

Coral reefs, which are nature's submerged breakwaters, are increasingly obliterated thus depriving coastal protection and marine life support. It does not help that reefs take a relatively long time to regenerate. The Reef Check 2010 annual report rates Malaysia's live coral cover as "fair" (scoring 44.3 %). The low percentage is of concern, given the rise in pollution from increased tourist development in the east coast of the Peninsula (Reef Check Foundation).

Over the years, various designs and performances of submerged breakwaters had been published; such as Reef Balls, BeachSaver Reefs and more recently, the Oyster Shell Bag Breakwaters. There are of course mixed reviews of all designs out there; hence lies the endless potentials in terms of improvement – both structural and performance wise.

Few researches have been done on staggered vertical submerged breakwaters. This study is undertaken to determine the design characteristic of the model and identify the performance limit of this newly developed breakwater shape.

## **1.3 Objectives and Scope of Study**

This study is intended to achieve the following outcomes: (i) to obtain experimental data and wave attenuating abilities ( $K_t$ ) of the model, subjected to regular and random waves in varying wave and parameters; and (ii) to compare experimental results with theoretical values. Tests are conducted with varying water depth, wave height, wave frequency and model porosity.

#### **1.4 Relevancy of Study**

The successful design and implementation of the M-Sub would contribute as an alternative solution to: (i) the stabilization of a coastline whilst without harm inflicted on the environment; (ii) a more economically viable and safer physical coastal development; and (iii) an improved marine habitat, indirectly boasting tourism. There have been mixed reviews on the current array of submerged breakwaters in the market. Hence, there is definitely room for innovations.

#### **1.5 Feasibility of Study within the Scope and Time Frame**

The study is expected to be feasible after deliberation based on the below:

- All laboratory equipment is readily available at the university labs;
- Help is easily accessible as laboratory assistants are very cooperative and experienced; and
- The scope consists of the studying of transmission coefficients and effects of porosity of the experimental models. The form of this research is straight forward and experimental-based.

## CHAPTER 2

### LITERATURE REVIEW

The first part of this chapter discusses the wave mechanics involved in this study, followed by the characteristics of submerged breakwaters as well a brief review of previous experimental studies related to the subject. Submerged breakwaters are also known as low crested breakwaters and reef breakwaters in various literature reviews.

#### 2.1 Wave Mechanics

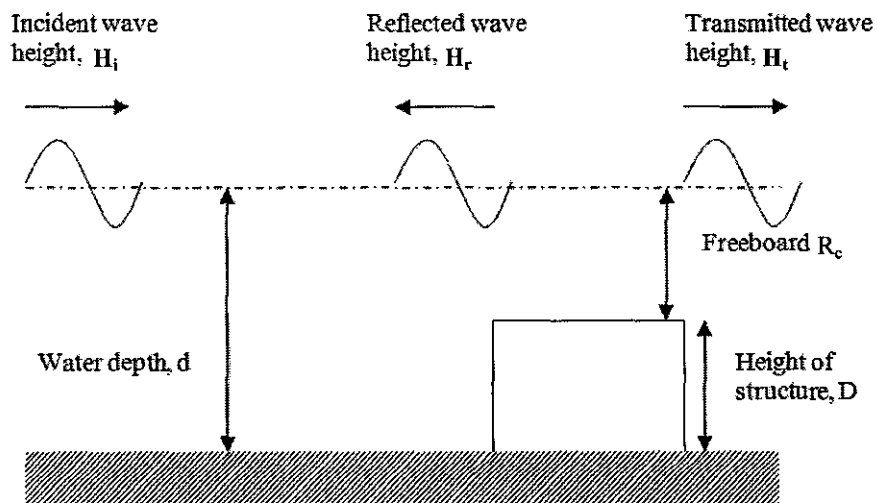


Figure 1: Wave mechanics and important connotations of a submerged breakwater

A single submerged breakwater as illustrated in Figure 1 is subjected to an incoming incident wave of height,  $H_i$ . Some part of the incident wave will be reflected to the seaward of the submerged structure in the form of reflected wave, with a height of  $H_r$  while some will be transmitted at the leeside as transmitted wave. The remaining energy will be dissipated at the structure through friction due to surface roughness, heat, sound and turbulence.

$H_i$  is usually taken as  $H_s$ . In depth limited waters (nearshore zones); the highest wave would break and not be subjected by the Rayleigh distribution anymore. The actual values used for wave heights in such cases are often 2 % wave height and  $H_{1/10}$  (Palmer, 1998).

$$\frac{H_{\max}}{H_{1/3}} = 1.45 \quad \text{and} \quad \frac{H_{\max}}{H_{1/10}} = 1.3 \quad (\text{Eq. 1})$$

Besides that, design breaker index  $H_b/d_b$  is important in determining placement of the submerged breakwater. For a gentle slope, the maximum ratio of  $H_b/d_b = 0.78$  is commonly used for wave breaking criteria, and decreases as the bottom slope increases (U.S. Army Corps of Engineers, 1984). These two parameters above are quite important in the design of submerged breakwaters.

## 2.2 Characteristics of a Nearshore Submerged Breakwater

The main effect of a submerged breakwater is that energy can pass over the crest and generate milder waves behind the structure, with less impact on the marine environment and ecology (Herbich, 2000). The efficiency of the structure and the resulting shoreline response mainly depend on transmission characteristics and the geometry of the structure.

Up to 40 countries around the world have constructed reef breakwaters (Baine, 2001).

Their purpose is to reduce hydraulic loading to maintain the dynamic equilibrium of a shoreline by allowing certain amount of wave energy transmission and dissipation (Pilarczyk, 2003). They are also intended for the enhancement of recreational and commercial fishing and mitigation of habitat loss and damage.

Popular offshore reef breakwaters in Malaysia range from used tires and fishing vessels (prior to the year 2006) to Tetrapod, Reefballs, and Hex Reefs (after the year 2006).

### 2.2.1. Transmission Characteristics

The effectiveness of a breakwater in attenuating wave energy can be measured by the amount of wave energy that is transmitted past the structure. Wave transmission is quantified by the use of the wave transmission coefficient.

For most existing design concepts, the energy of the wave spectrum in front of the submerged breakwater is compared to the energy of the spectrum behind the reef by means of the transmission coefficient,  $K_t$ .

The greater the wave transmission coefficient, the weaker the wave attenuation. As defined in Equation 2 below,  $K_t$  has a range of  $0 < K_t < 1$ . A value of 0 implies no transmission (high, impermeable structure) and a value of 1 implies complete transmission (no structure).

$$K_t = \frac{H_t}{H_i} = \sqrt{\frac{E_t}{E_i}} \quad (\text{Eq. 2})$$

Where  $H_i$  = incident wave height;

$E_i$  = incident wave energy;

$H_t$  = transmitted wave height;

$E_t$  = transmitted wave energy

Pilarczyk (2003) and Black (2003) outlined a formula to determine the wave transmission coefficient  $K_t$  for different values of relative crest width,  $B/L$ , and crest height,  $R_c/H_i$ .

- $B/L$  is the relative structure length characterizing the wave's residence time on reef (resonance criterion). It is a ratio of structure width over wave length; and
- $R_c/H_i$  being relative water depth above the reef representing a non-linearity parameter for shallow water (also known as shallow water breaking criterion). It is a ratio of crest freeboard over incident wave height.

Another formula in determining wave transmission over a submerged structure is studied by d'Angremond et al. (1996).

The formula is given by Eq.3:

$$K_t = -0.4 \frac{R_c}{H_i} + C \left( \frac{B}{H_i} \right)^{-0.31} (1 - e^{-0.5\xi}) \quad (\text{Eq. 3})$$

Where  $R_c$  = Crest freeboard (m)

$C = 0.64$  for a permeable structure

$B$  = Crest width (m)

$C = 0.80$  for an impermeable structure

$\xi$  = Surf similarity parameter

Through this study, it was observed that there is a good agreement between the calculated wave transmission and the measured one. This formula was implemented for the Amwaj Islands Development Project in Bahrain. New islands were to be built on the existing coral reef. Hence, to protect the waterfront developments on the mentioned island from wave attack a submerged breakwater was proposed.

Figure 2 and Figure 3 in the following pages demonstrate how the performance (in terms of wave transmission) of a submerged structure depended on the ratio  $B/L$  and  $R_c/H_i$ . As observed, decreasing these ratios would increase the transmission and hence, affecting the performance of the structure.

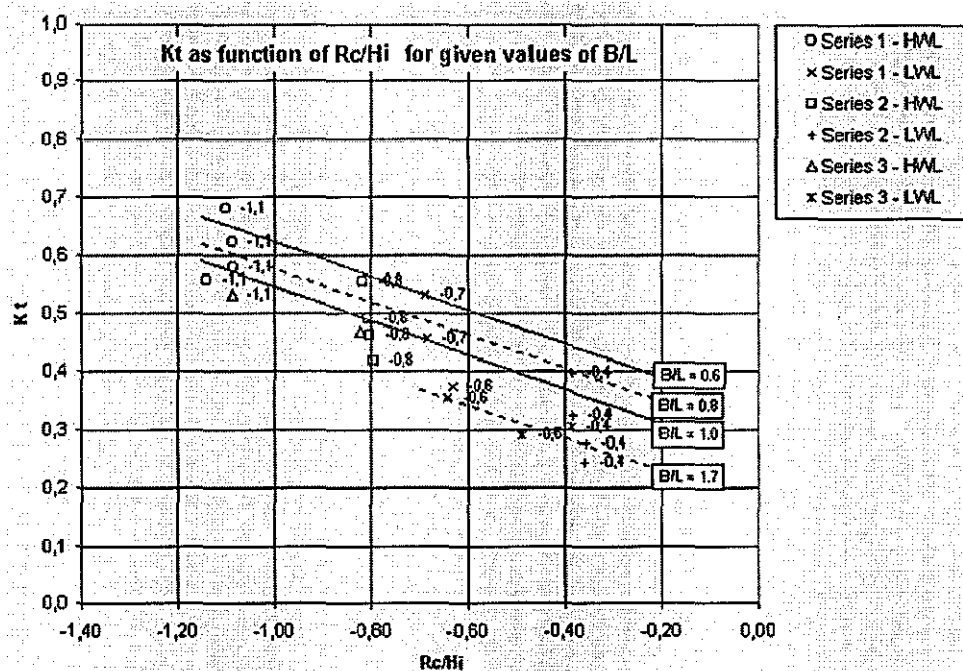


Figure 2: Graph of  $K_t$  as a function of  $R_c/H_i$  for given values of  $B/L$ .

Source: Pilarczyk, 2003

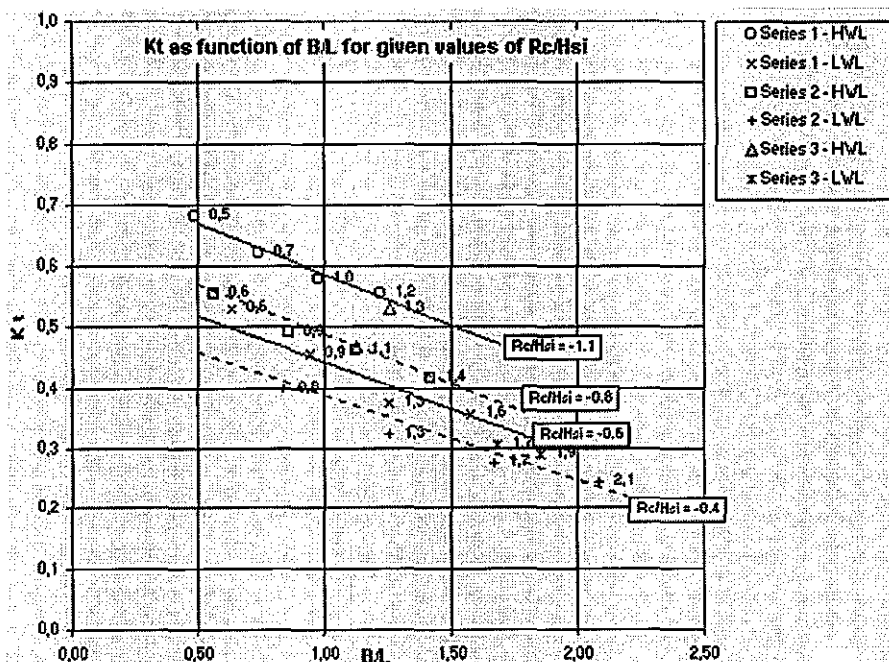


Figure 3: Graph of  $K_t$  as a function of  $B/L$  for given values of  $R_c/H_i$ .

Source: Pilarczyk, 2003

Hydraulic model test results measured by Seelig (1980), Powell and Allsop (1985), Daemrich and Kahle (1985), Ahrens (1987) and Van der Meer (1998a) resulted in a

single prediction method. Similarly, they all related  $K_t$  to the relative crest freeboard,  $R_c/H_i$ . The data used is plotted as such in Figure 4.

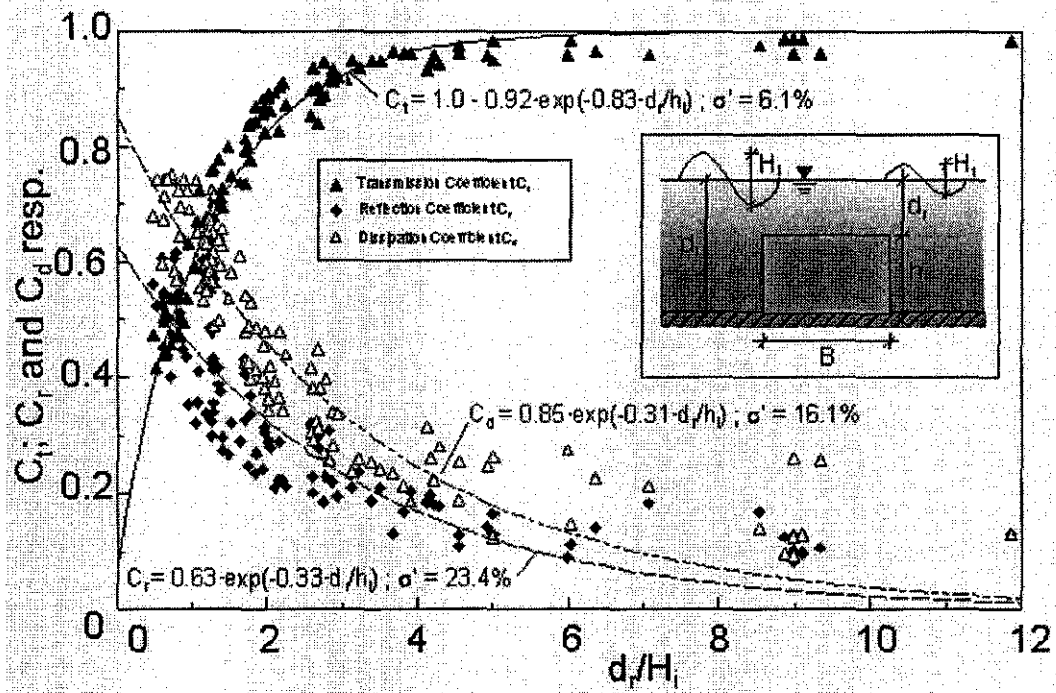


Figure 4: Graphs of  $d_f/H_i$  in relation to  $C_t$ ,  $C_r$  and  $C_d$ . Source: Bleck, 2006

The graphs above show  $R_c/H_i$  (represented as  $d_f/H_i$  in Figure 4) is the most accurate in determining  $K_t$  (represented as  $C_t$  in Figure 4) in relevance to  $C_r/K_R$  (reflection coefficient) and  $C_d/K_D$  (dissipation coefficient).

The Coastal Engineering Manual (2002) provides information on how to calculate the transmission coefficient using equations formulated by Van der Meer (U.S. Army Corps of Engineers, 2002). The equations given by Van der Meer et al. (2005) are a continuation of previous literature published by d'Angremond et al. (1996) and Van der Meer and d'Angremond (1992).

The formulae depend primarily upon non-dimensional relationships between the incident wave height and the physical characteristics of the structure. The final equations published in Van der Meer et al. (2005) are shown below.

For  $\frac{B}{H_i} < 8$ , 
$$K_t = -0.40 \frac{R_c}{H_i} + 0.64 \left(\frac{B}{H_i}\right)^{-0.31} (1 - e^{-0.50\xi}) \quad (\text{Eq. 4})$$

For  $\frac{B}{H_i} > 12$ , 
$$K_t = -0.35 \frac{R_c}{H_i} + 0.51 \left(\frac{B}{H_i}\right)^{-0.65} (1 - e^{-0.41\xi}) \quad (\text{Eq. 5})$$

The gap that exists in the range  $8 < B/H_i < 12$ , where the Van der Meer et al. (2005) equations give a discontinuity in this range. It is suggested that linear interpolation is used for values of  $B/H_i$  that fall within this range. Additionally, Van der Meer et al. (2005) suggests limits for the maximum and minimum values of  $K_t$ . The lower limit,  $K_{t,l}$ , is defined as a constant 0.05. The upper limit  $K_{t,u}$ , is given a linear dependency on  $B/H_i$ .

### 2.2.2. Porosity

Sidek (2007) addressed how variation of porosity of a submerged permeable breakwater affects non-breaking wave transformation.

Porosity here is defined as the volume of empty space in a model divided by the total geometrical volume of the test model. Table 1 illustrates the physical dimensions of the test models.

Table 1 : Dimensions of individual test model unit

| Model Unit Type | Porosity | Gap Size (cm) |
|-----------------|----------|---------------|
| 1               | 0.4      | 2.4           |
| 2               | 0.6      | 5.8           |
| 3               | 0.8      | 17.8          |

Important observations made during the study were:

- The less porous models correspond to a larger  $K_r$  but smaller  $K_t$  and vice versa.
- The less porous models tend to dissipate greater wave energy. Energy loss was higher when porosity decreased at small  $k_d$  values. However, this was not so obvious when  $k_d$  values were larger.

Table 2 compares the results of this study with one done in 2004, illustrating the effects of porosity on  $K_t$ ,  $K_r$ , and  $K_d$ .

Table 2: Comparison of results between two porosity studies

| Results from Sidek (2007) for<br>F/d = 0.3 |           |           |           | Results from Ting et al. (2004) for<br>F/d = 0.2 |           |           |           |
|--|-----------|-----------|-----------|--|-----------|-----------|-----------|
| Porosity                                   | $K_t$     | $K_r$     | $K_d$     | Porosity   | $K_t$     | $K_r$     | $K_d$     |
| 0.4  | 0.37-0.57 | 0.11-0.31 | 0.79-0.92 | 0.42   | 0.50-0.76 | 0.05-0.30 | 0.63-0.83 |
| 0.6  | 0.44-0.60 | 0.06-0.27 | 0.77-0.89 | 0.59   | 0.63-0.80 | 0.01-0.19 | 0.59-0.77 |
| 0.8  | 0.53-0.71 | 0.01-0.24 | 0.71-0.83 | 0.81   | 0.73-0.84 | 0.02-0.10 | 0.53-0.68 |

Both studies show similar trends. They both observed that there is an increase in  $K_t$  when porosity increased. Simply put, the more porous test models were more effective in transmitting waves. On the other hand,  $K_r$  and  $K_d$  decrease with the increase in porosity values.

### 2.3. Characteristics of a Fish Habitat Enhancer

As one of the intended functions of the M-Sub is similar to that of an artificial reef, its characteristics are comparable to the latter.

Corals are Cnidarians, the same phylum as anemones and jellyfish. However, unlike jellyfish and anemones, "scleractinian" or stony corals leaves a calcium carbonate skeleton when the coral dies. A coral reef is the result of the steady build-up of corals on the surface forming calcified remains (Wildasia Org, 2005). Artificial reefs (ARs) have been defined as "any material purposely placed in the marine environment to influence physical, biological, or socio-economic processes related to living marine organisms" (Bushnell, 2007).

The construction of an artificial reef may greatly alter the environmental conditions of an area. The Japanese have used artificial reefs in deep and calm waters to deflect horizontal ocean currents upwards, thereby inducing upwelling (Grove and Sonu, 1983). Upwelling brings the deeper, colder nutrient water to the surface, which in turn increases the biological productivity of the surface waters.

There is a number of elements influencing recruitment and colonisation of a reef breakwater. In general, they are categorized according to environment characteristics, reef characteristics and biotic influences.

#### Environment characteristics

The Great Barrier Reef, owes its abundance of life to the warm waters, ample amount of light exposure, and salt waters of Australia. The following are vital aspects of environment factors of the design of artificial reefs.

- Location

Diversity at natural reefs tend to increase closer to the equator and vary vastly between the northern and southern hemisphere (Moreno and Jara, 1984). Cases where ARs do not enhance species number is mostly due to the natural scarcity of species in the region. Factors such as distance from the shore, other reefs and geological features would also greatly influence the variety of organisms and their distribution.

- Depth/water column

The performance of ARs as fisheries habitat was found to be highly dependent on the depth of deployment (Jara and Cespedes, 1994). This is due to the vast changes in temperature, salinity, turbidity and light across a vertical water column, which in turn affects the changes in plankton components with influences the presences of many species (Bortone et al., 2000).

- Substrate

Reef species feed in sediment dwelling animals surrounding the reefs. Hence the nature of substrate determines the infaunal composition and type of food available. That aside, substrate gradation would influence sediment resuspension due to water motion. In areas of fine sediments, low ARs possibly might be covered by silt particles, discouraging algal and invertebrate settlement (Golani and Diamant 1999).

#### Reef characteristics

- Materials and dimensions

Generally, structures that lack habitat complexity would be less favorable to tiny organisms due to lack of protection from preys. Therefore, it was often observed

that the number of species present at a rock structure is more significant than that of a geo-container.

Bohnsack et al. (1994) found that larger ARs are possibly better for fishing while smaller ARs are more effective in overall recruitment. This would probably be due to the larger ratio between reef volume and surface area.

### Biotic aspects

Colonisation of a reef is very much dependent of the in situ ecology. Biotics influences range from individual to population to to assemblage level (Bortone et al., 2000).

As this M-Sub doubles as an wave attenuator, the aquatic environment surrounding it is more turbulent than the typical AR. A study done by Cummings (1994) of a shallow water reef in Florida indicated that a community of fish sprouted within 3 months after placement. However, observations of algae and invertebrates as well as true succession of the community were not as positive. Cummings concluded that the frequent physical disturbances by waves and insufficient study duration were not adequate in assessing the performance of shallow reefs.

## **CHAPTER 3**

### **METHODOLOGY**

#### **3.1 Project Activities**

Two methods have been employed throughout the course of this research: (1) theoretical analysis using the 1996 d'Angremond et al. formula to estimate the performance of the model; and (2) experimental works, which purposes are to collect data to verify the calculated theoretical outputs. Figure 5 describes the overall methodology and general flow of this project, whereas Figure 6 illustrates the setting of the experiment.

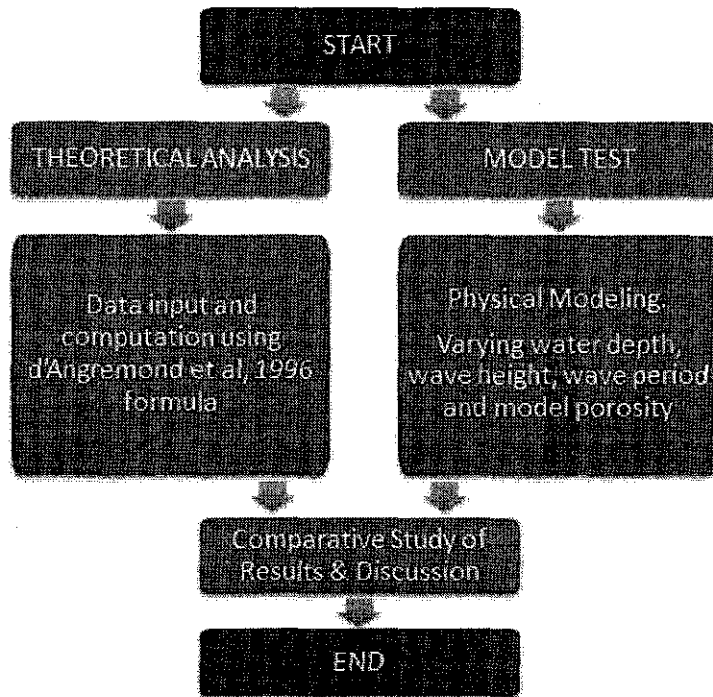


Figure 5: Methodology and general flow of the study

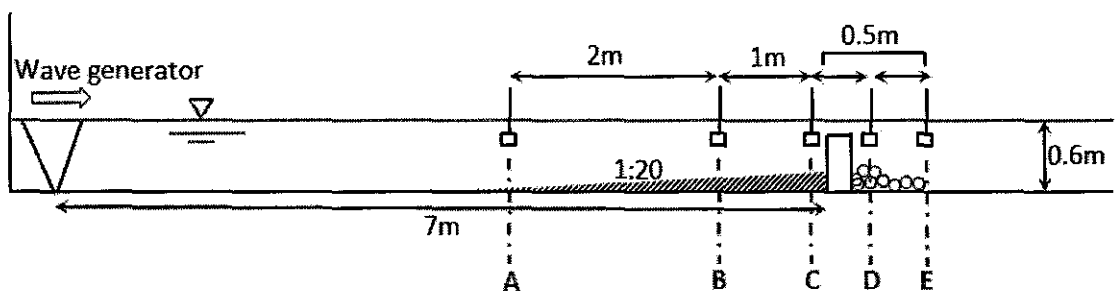


Figure 6: Experimental settings. A, B, C, D and E denotes the location of wave gauges

The experimental work conducted in the study is designed to measure the transmitted wave height,  $H_t$ , which is attenuated by the scaled down structure at wave gauge D. To simplify testing and analysis, the incident wave height is measured as the wave height produced by the wave generator 3 m prior to the placement of the model (wave gauge A) in the testing area. The transmission coefficient,  $K_t$ , is measured by

the ratio of the transmitted wave height to the incident wave height and is reported as a dimensionless parameter (Eq. 2).

Monochromatic regular and irregular waves were used throughout the tests. The experimental works involved 144 unique combinations of varying parameters for sets of non-porous model and porous model, excluding calibration runs. The depth of the water was varied among 0.60 m, 0.65 m and 0.70 m. The incident wave height and incident wave period were also varied for each water depth. Table 3 shows the various wave characteristics used in the study.

Table 3: Wave characteristics employed in the study

| Test | Wave Height<br>(m) | Wave Period<br>(s) | $H_i/gT^2$ |         |
|------|--------------------|--------------------|------------|---------|
| 1    | 0.2                | 1.118              | 0.0163     | Regular |
| 2    | 0.2                | 1.342              | 0.0113     |         |
| 3    | 0.2                | 1.565              | 0.0083     |         |
| 4    | 0.18               | 1.118              | 0.0147     |         |
| 5    | 0.18               | 1.342              | 0.0109     |         |
| 6    | 0.18               | 1.565              | 0.0749     |         |
| 7    | 0.16               | 1.118              | 0.0131     |         |
| 8    | 0.16               | 1.342              | 0.0091     |         |
| 9    | 0.16               | 1.565              | 0.0067     |         |
| 10   | 0.3                | 1.657              | 0.0111     | Random  |
| 11   | 0.26               | 1.543              | 0.0111     |         |
| 12   | 0.22               | 1.419              | 0.0111     |         |

Water Depth (m) : 0.6, 0.65, 0.70

### 3.2 Equipment and Tools

A series of physical modelling tests carried out in the Offshore Laboratory of Universiti Teknologi PETRONAS. The tests were conducted in wave-only conditions in a 23 m in total length, 1.5 m wide and 1.5 m high wave flume, the main equipment of the study, as shown in Figure 7 below.

The flume walls have three 15 mm glass panelled windows where models are constructed, which allows visual observations to be made throughout testing. The permanent floor of the flume is constructed of concrete, although site specific two dimensional bathymetric profiles could be reproduced in the flume using false flooring/gravels.

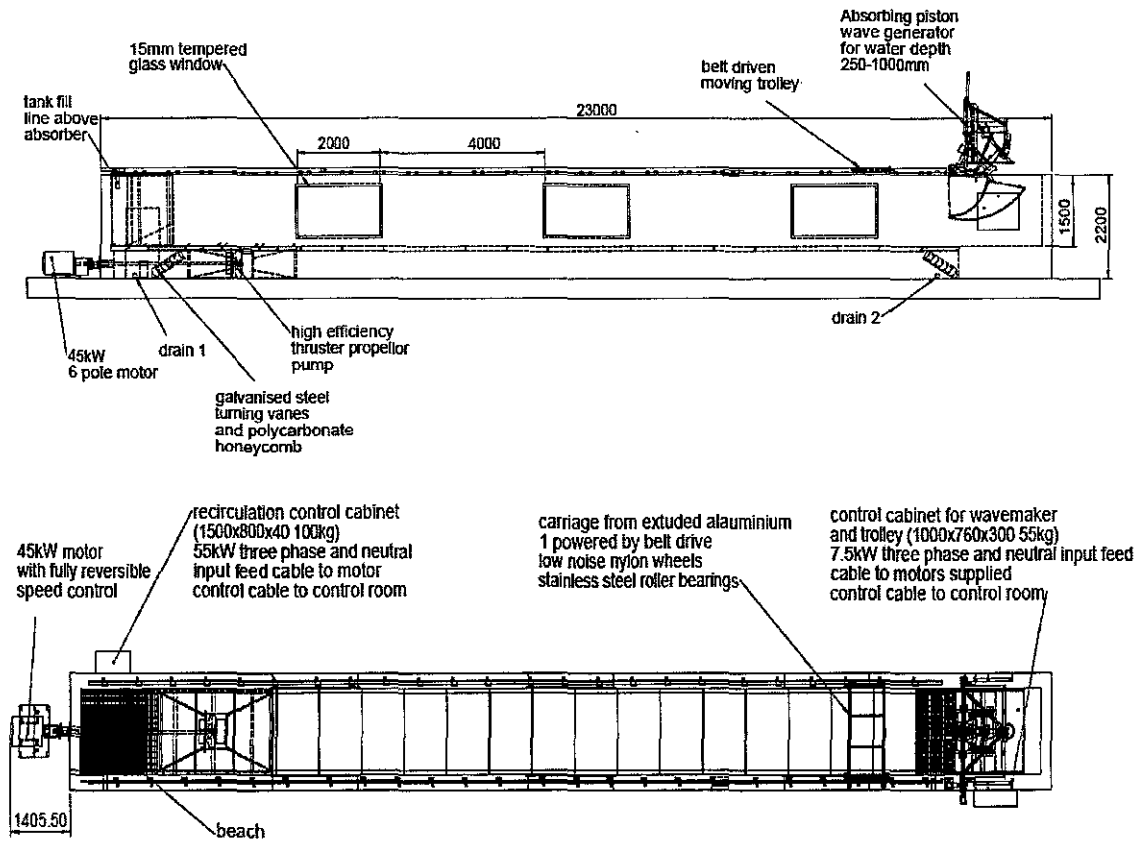


Figure 7 : (Above) Side view and (Below) Plan view of the wave flume used for this study

At one end of the flow channel is a piston-type wave generator and at the other end is a wave absorber to reduce the reflection of waves resulted from the reflective boundary of the flume. The wave flume is complemented by HR Wallingford, a software suite providing a complete package for defining, running and processing the results of the experiments.

Prior to the experiments, the model were constructed at the Concrete Lab of UTP with available concreting materials and devices. A total of 160 individual grade 40

concrete breakwaters were casted and cured for 28 days. Figure 8 describes the dimensions of model units whereas Figure 9 demonstrates the configuration of breakwater utilized throughout the study

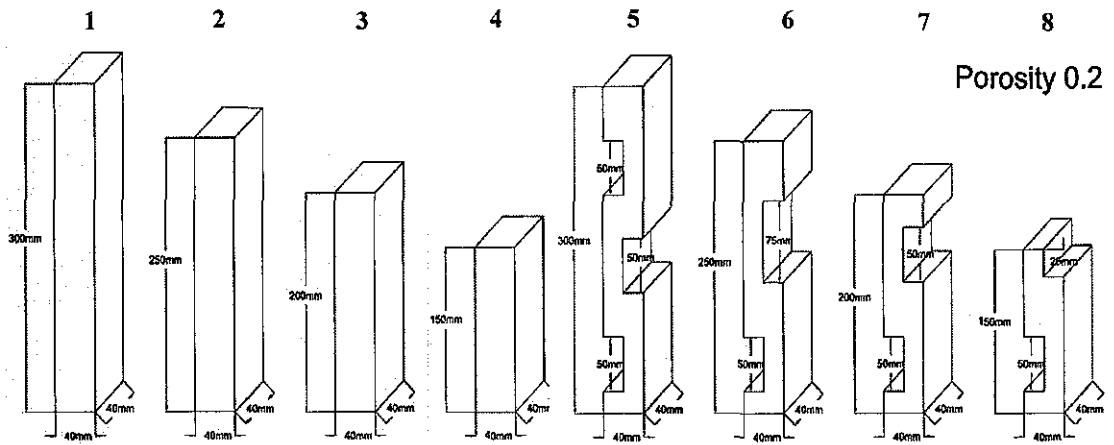


Figure 8: Different units of the two types of model breakwater

Units 1, 2, 3 and 4 make up the non-porous model. On the other hand, units 5, 6, 7, and 8 make up the porous model. There are a total of 150 of such units in each model.

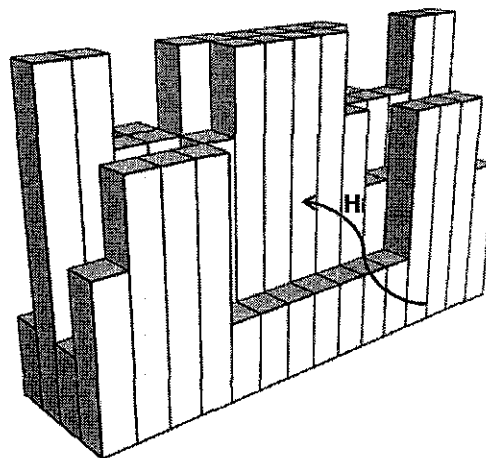


Figure 9: Configuration of the breakwater model



## CHAPTER 4

### RESULTS AND DISCUSSION

All wave data captured were analysed using short term wave analysis by utilizing time domain. In time domain analysis, zero crossing method is used to obtain individual wave height for a series of wave.

The results obtained from the experiments conducted can be divided into theoretical and measured data. The theoretical results were determined using Eq. 3 while the measured results were plotted based on the raw data of the wave gauge.

$$K_t = -0.4 \frac{R_c}{H_i} + C \left( \frac{B}{H_i} \right)^{-0.31} (1 - e^{-0.5\xi}) \quad (\text{Eq. 3})$$

To obtain measured transmission coefficient, the ratio of the transmitted wave height to the incident wave height is computed and is reported as a dimensionless parameter (Eq. 2).

This chapter discusses the results according to the water depths employed for the experiments.

#### 4.1 Results for 0.70 m water depth

Table 4 summarizes the wave parameters used as well as the theoretical transmission coefficient values for Non Porous ( $K_t 1$ ) and Porous ( $K_t 2$ ) Models.

Table 4: Summary of wave parameters and their corresponding transmission coefficient at water depth of 0.70 m

| Test | Wave Height (m) | Wave Period (s) | $H_i/gT^2$ | $R_c/H_i$ | $B/H_i$ | $B/L$  | $K_t, 1$ | $K_t, 2$ |         |
|------|-----------------|-----------------|------------|-----------|---------|--------|----------|----------|---------|
| 1    | 0.2             | 1.118           | 0.0163     | -1.375    | 0.2     | 0.0205 | 1.1212   | 1.007    | Regular |
| 2    | 0.2             | 1.342           | 0.0113     | -1.375    | 0.2     | 0.0142 | 1.2014   | 1.071    |         |
| 3    | 0.2             | 1.565           | 0.0083     | -1.375    | 0.2     | 0.0105 | 1.2730   | 1.128    |         |
| 4    | 0.18            | 1.118           | 0.0147     | -1.528    | 0.222   | 0.0205 | 1.1859   | 1.071    |         |
| 5    | 0.18            | 1.342           | 0.0109     | -1.528    | 0.222   | 0.0142 | 1.2650   | 1.134    |         |
| 6    | 0.18            | 1.565           | 0.0749     | -1.528    | 0.222   | 0.0105 | 1.3351   | 1.190    |         |
| 7    | 0.16            | 1.118           | 0.0131     | -1.719    | 0.25    | 0.0205 | 1.2657   | 1.150    |         |
| 8    | 0.16            | 1.342           | 0.0091     | -1.719    | 0.25    | 0.0142 | 1.3435   | 1.212    |         |
| 9    | 0.16            | 1.565           | 0.0067     | -1.719    | 0.25    | 0.0105 | 1.4119   | 1.267    |         |
| 10   | 0.3             | 1.657           | 0.0111     | -0.917    | 0.133   | 0.0093 | 1.1098   | 0.961    | Random  |
| 11   | 0.26            | 1.543           | 0.0111     | -1.058    | 0.154   | 0.0108 | 1.1340   | 0.992    |         |
| 12   | 0.22            | 1.419           | 0.0111     | -1.250    | 0.182   | 0.0127 | 1.1750   | 1.040    |         |

As speculated, the theoretical transmission coefficient of the second model is much lower for both regular and random wave. The difference in performance was noted to be between 9.1 %-13.4 %\*.

\* All computations of percentage differences employ the formula of Percentage Difference =  $(K_{t1} - K_{t2})/K_{t1}$

Tables 5 and 6 in the next page summarize the experimental results for both non-porous and porous models.

Table 5: Experimental results for non-porous model ( $K_t$  1) at water depth 0.70 m

|        | Wave Gauge |            |            |            |            | $K_t$ 1 |         |
|--------|------------|------------|------------|------------|------------|---------|---------|
|        | A          | B          | C          | D          | E          |         |         |
|        | $H_s$ (mm) |         |         |
| Test1  | 161.423    | 158.838    | 144.729    | 140.597    | 151.766    | 0.8966  | Regular |
| Test2  | 163.863    | 154.984    | 165.14     | 139.588    | 155.82     | 1.0078  |         |
| Test3  | 136.734    | 197.671    | 149.504    | 166.524    | 166.668    | 1.0934  |         |
| Test4  | 187.047    | 162.609    | 146.069    | 150.448    | 148.166    | 0.7809  |         |
| Test 5 | 185.332    | 172.143    | 177.474    | 143.858    | 171.19     | 0.9576  |         |
| Test6  | 152.138    | 219.14     | 161.044    | 190.5      | 180.947    | 1.0585  |         |
| Test7  | 199.509    | 181.743    | 165.103    | 150.004    | 157.536    | 0.8275  |         |
| Test8  | 208.114    | 187.011    | 190.379    | 155.568    | 189.599    | 0.9148  |         |
| Test9  | 165.147    | 242.025    | 169.892    | 211.55     | 191.383    | 1.0287  |         |
| Test10 | 105.8      | 119.0225   | 102.566    | 98.081     | 99.301     | 0.9694  | Random  |
| Test11 | 88.73      | 93.5215    | 84.237     | 80.743     | 82.129     | 0.9494  |         |
| Test12 | 76.011     | 77.682     | 70.529     | 66.6       | 68.3435    | 0.9279  |         |

Table 6: Experimental results for porous model ( $K_t$  2) at water depth 0.70 m

|        | Wave Gauge |            |            |            |            | $K_t$ 2 |         |
|--------|------------|------------|------------|------------|------------|---------|---------|
|        | A          | B          | C          | D          | E          |         |         |
|        | $H_s$ (mm) |         |         |
| Test1  | 161.365    | 157.107    | 156.801    | 136.484    | 155.291    | 0.9624  | Regular |
| Test2  | 169.157    | 163.07     | 152.695    | 160.614    | 139.739    | 0.8261  |         |
| Test3  | 151.466    | 112.459    | 155.03     | 122.736    | 129.028    | 0.8519  |         |
| Test4  | 176.152    | 181.597    | 170.62     | 153.944    | 160.483    | 0.9110  |         |
| Test 5 | 176.388    | 183.577    | 171.541    | 157.349    | 158.398    | 0.8980  |         |
| Test6  | 172.297    | 127.215    | 175.165    | 140.122    | 147.758    | 0.8576  |         |
| Test7  | 191.765    | 197.901    | 182.219    | 162.584    | 164.637    | 0.8585  |         |
| Test8  | 203.885    | 200.063    | 177.436    | 179.154    | 148.081    | 0.7263  |         |
| Test9  | 192.619    | 141.903    | 197.532    | 155.259    | 162.44     | 0.8433  |         |
| Test10 | 107.7225   | 102.896    | 114.664    | 99.4615    | 94.096     | 0.8735  | Random  |
| Test11 | 92.52      | 90.257     | 95.3735    | 84.0455    | 80.561     | 0.8707  |         |
| Test12 | 76.493     | 76.4815    | 77.9745    | 69.2045    | 66.338     | 0.8672  |         |

Figure 11 and Figure 12 on the following pages describes  $K_t$  as a function of  $B/L$ , given  $R_c/H_i$  for regular and random wave conditions respectively at water depth 0.70 m. 'T' denotes theoretical values whereas 'E' denotes experimental results.

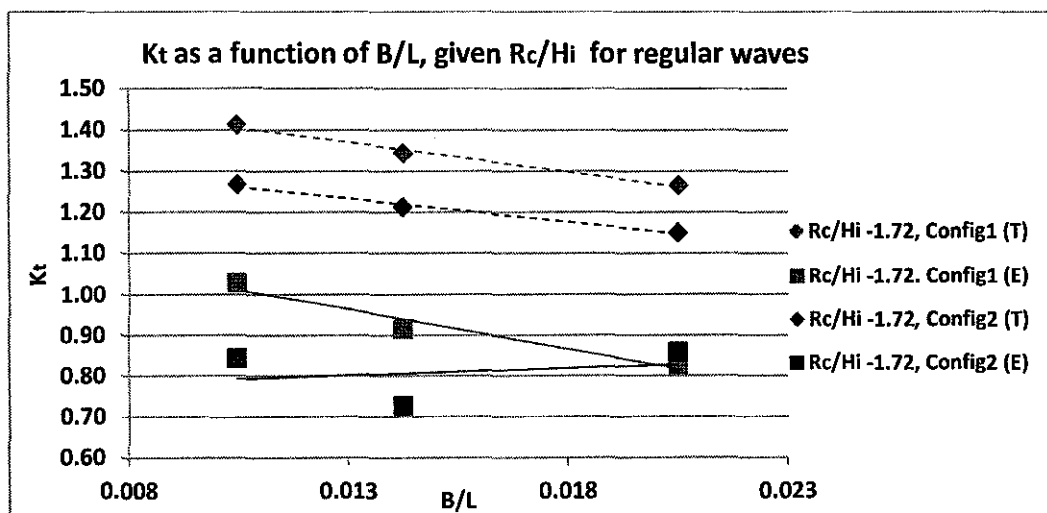
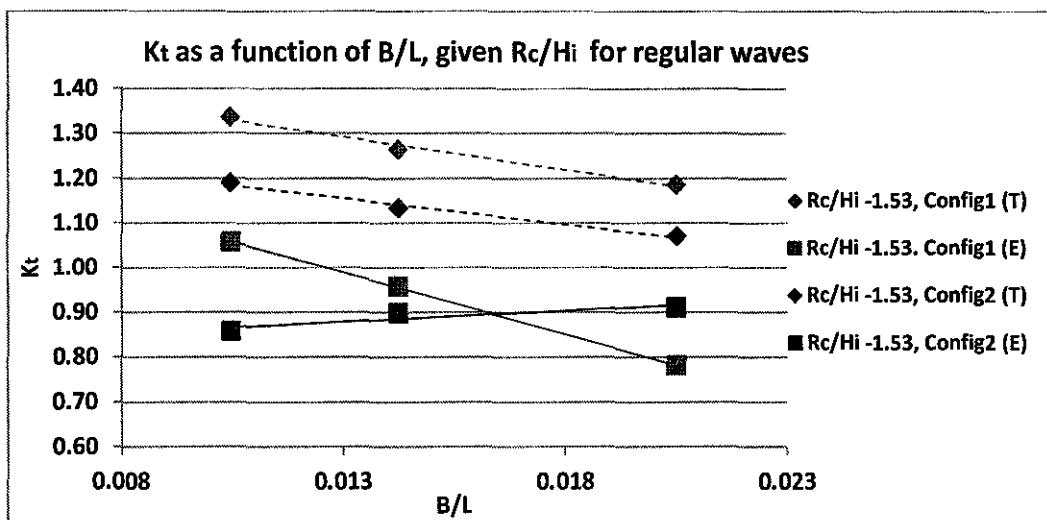
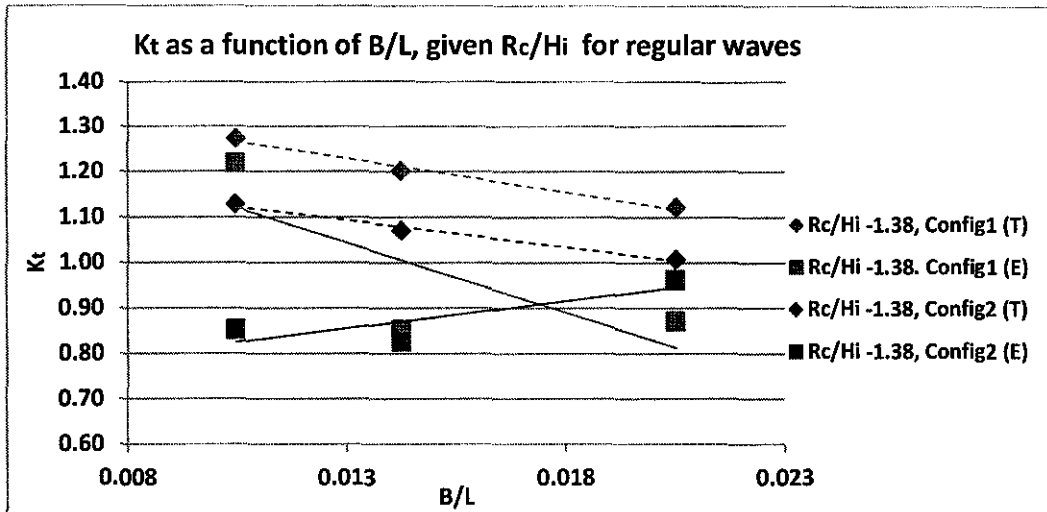


Figure 11 : K<sub>t</sub> as a function of B/L, given R<sub>c</sub>/H<sub>i</sub> for regular wave conditions  
(d=0.70 m)

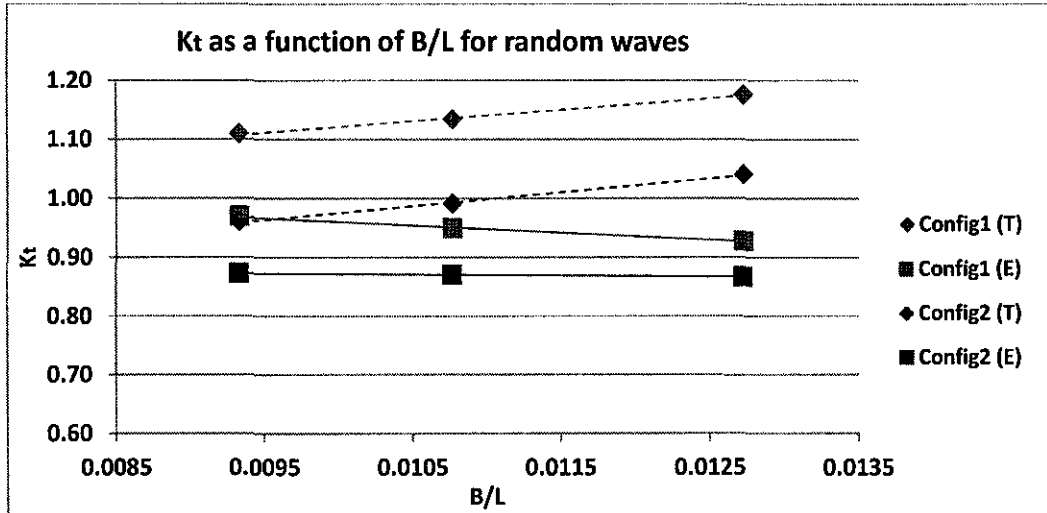


Figure 12:  $K_t$  as a function of  $B/L$ , given  $R_c/H_i$  for random wave conditions  
( $d=0.70$  m)

The lowest transmission coefficient observed experimentally for the non-porous configuration is 0.78, which translate to a maximum wave reduction of 22%. As for the porous configuration, the lowest transmission coefficient observed is 0.73.

For both random and regular waves, the plots show a consistent range and trend of data. It is observed that a relatively high correlation exist between the theoretical and experimental  $K_t$  for the non-porous set. A lower transmission coefficient is mostly achieved as  $B/L$  increases. Simply put, as the relative structure length increases, dissipative abilities of the model increases.

This means that, the breakwater reduces the transmitted waves as the breakwater width ( $B$ ) increases or the wave length ( $L$ ) decreases. This behaviour could be due to; (i) the increase of the breakwater width causes the increase of the friction between the breakwater surface and the transmitted waves, causing more wave energy loss; and (or) (ii) as the wave becomes short, the water particle velocity and acceleration suddenly change and addition turbulence due to this sudden change causes dissipation in the wave energy.

However, trend for the experimental data of the porous set is not as highly coherent as its non-porous counterpart, especially for runs involving regular waves. Due to conditions at  $B/L = 0.0205$  of this model set, its experimental

results show an inverse of its expected values. This finding is unanticipated as given the same breakwater width; a higher  $B/L$  value dictates a shorter wavelength passing through, hence in theory, better wave dissipative abilities. The reason behind this phenomenon could possibly be due to the complex shape of the model and its porosity. Turbulences generated after the breakwater might not be sufficient in causing great reduction in the wave energy behind the structure.

Figure 13 on the following page describes  $K_t$  as a function of  $R_c/H_i$ , given  $B/L$  for regular wave conditions at water depth 0.70 m, whereas Figure 14 describes the relationship of  $K_t$  and  $R_c/H_i$ , given  $B/L$  for regular wave conditions at water depth 0.70 m.

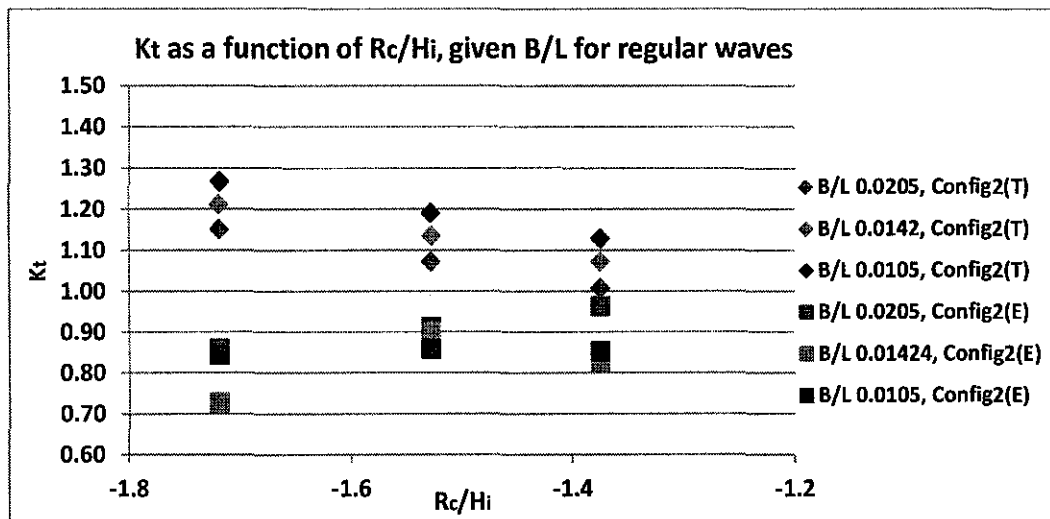
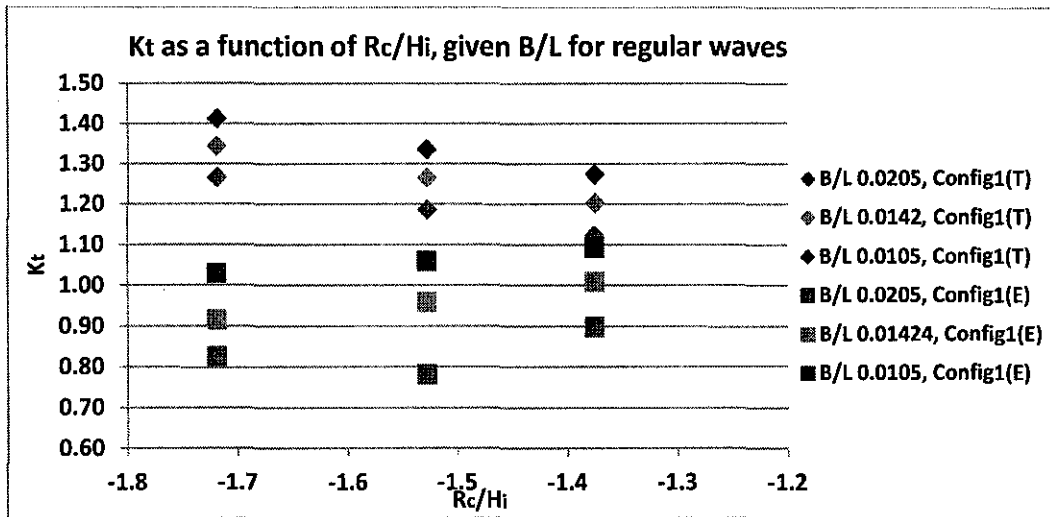


Figure 13: K<sub>t</sub> as a function of R<sub>c</sub>/H<sub>i</sub> given B/L for regular wave conditions  
(d=0.70 m)

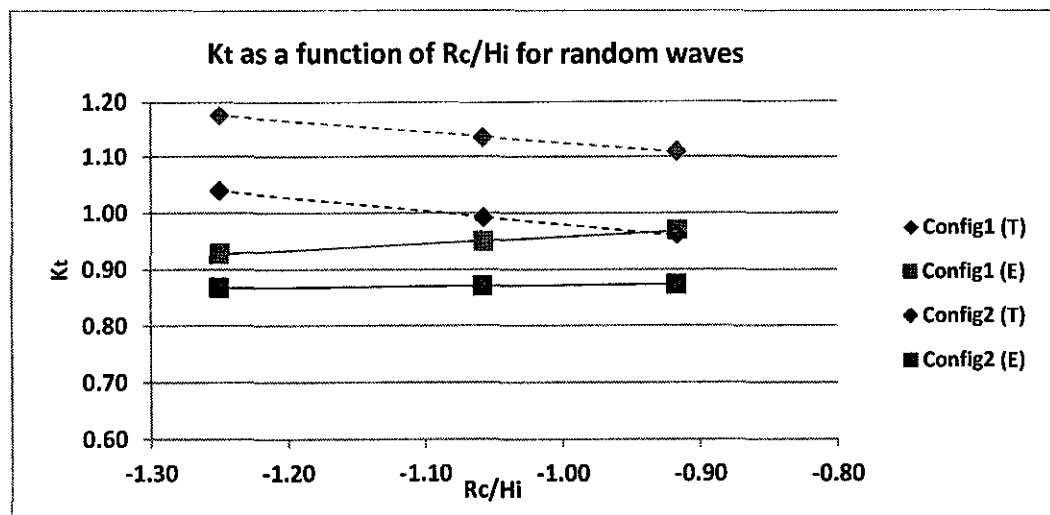


Figure 14: K<sub>t</sub> as a function of R<sub>c</sub>/H<sub>i</sub> given B/L for random wave conditions  
(d=0.70 m)

In theory, the lower the  $R_c/H_i$  value, the lower the relative transmission coefficient of the breakwater. In basic terms, often, the breakwater reduces the transmitted waves as the breakwater crest freeboard ( $R_c$ ) reduces. It could probably be due to the increase in wave height ( $H_i$ ) too.

This happens when the incident waves are ‘more in contact’ with the structure. Wave overtopping occurs rapidly as wave height reduces over the crest because of energy dissipation due to flow separation.

It is observed that a slight inverse coherence exist between the theoretical and experimental  $K_t$  for the both sets, possibly due to the complexity of the shape of the structure. Nevertheless, generally, for the both sets of breakwater, given a constant  $R_c/H_i$ , the higher the  $B/L$ , the lower the  $K_t$ .

Figure 15 and Figure 16 depict the comparison of  $K_t$  for both regular and random wave conditions at water depth 0.70 m.

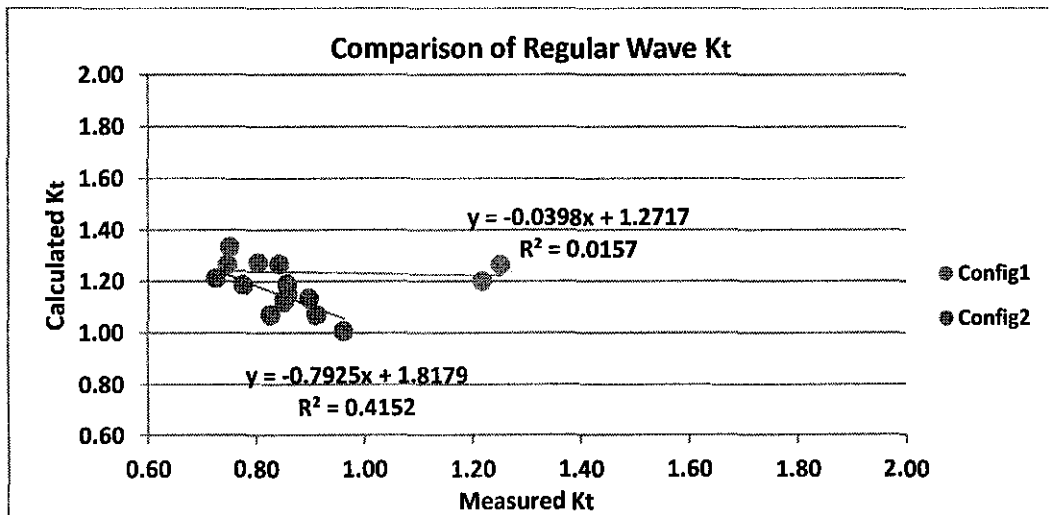


Figure 15: Comparison of calculated and measured  $K_t$  for regular wave conditions ( $d=0.70$  m)

The index of fit value ( $R^2$ ) was computed to be 0.02 and 0.42 for the non-porous and porous configuration respectively. This means that 2% of variability in  $K_t$  of the non-porous set can be explained by Eq.3 (shown below) and its governing parameters. Likewise for the other set.

$$K_t = -0.4 \frac{R_c}{H_t} + C \left( \frac{B}{H_t} \right)^{-0.31} (1 - e^{-0.5\xi})$$

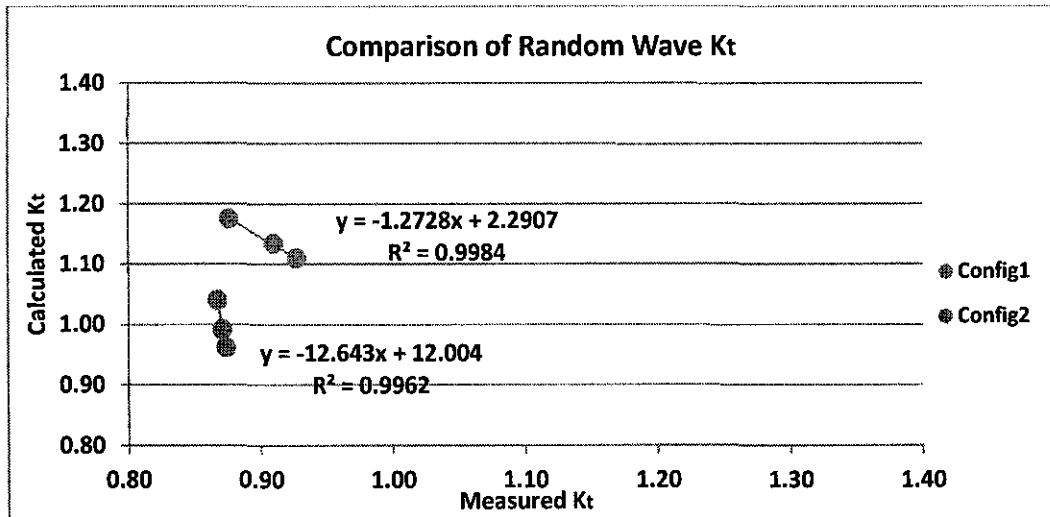


Figure 16: Comparison of calculated and measured  $K_t$  for random wave conditions ( $d=0.70$  m)

As for random waves, the index of fit value ( $R^2$ ) was computed to be 0.998 and 0.996 for the non-porous and porous configuration respectively.

## 4.2 Results for 0.65 m water depth

Table 7 summarizes the wave parameters used as well as the theoretical transmission coefficient values for Non Porous ( $K_t 1$ ) and Porous ( $K_t 2$ ) Models.

Table 7: Summary of wave parameters and their corresponding transmission coefficient at water depth of 0.65 m

| Test | Wave Height (m) | Wave Period (s) | $H_i/gT^2$ | $R_c/H_i$ | $B/H_i$ | $B/L$  | $K_t 1$ | $K_t 2$ |         |
|------|-----------------|-----------------|------------|-----------|---------|--------|---------|---------|---------|
| 1    | 0.2             | 1.118           | 0.0163     | -1.125    | 0.2     | 0.0205 | 1.0212  | 0.907   | Regular |
| 2    | 0.2             | 1.342           | 0.0113     | -1.125    | 0.2     | 0.0142 | 1.1014  | 0.971   |         |
| 3    | 0.2             | 1.565           | 0.0083     | -1.125    | 0.2     | 0.0105 | 1.1730  | 1.028   |         |
| 4    | 0.18            | 1.118           | 0.0147     | -1.25     | 0.222   | 0.0205 | 1.0747  | 0.960   |         |
| 5    | 0.18            | 1.342           | 0.0109     | -1.25     | 0.222   | 0.0142 | 1.1538  | 1.023   |         |
| 6    | 0.18            | 1.565           | 0.0749     | -1.25     | 0.222   | 0.0105 | 1.2240  | 1.079   |         |
| 7    | 0.16            | 1.118           | 0.0131     | -1.406    | 0.25    | 0.0205 | 1.1407  | 1.025   |         |
| 8    | 0.16            | 1.342           | 0.0091     | -1.406    | 0.25    | 0.0142 | 1.2185  | 1.087   |         |
| 9    | 0.16            | 1.565           | 0.0067     | -1.406    | 0.25    | 0.0105 | 1.2869  | 1.142   |         |
| 10   | 0.3             | 1.657           | 0.0111     | -0.75     | 0.1333  | 0.0093 | 1.0431  | 0.8945  | Random  |
| 11   | 0.26            | 1.543           | 0.0111     | -0.865    | 0.1538  | 0.0108 | 1.0571  | 0.9149  |         |
| 12   | 0.22            | 1.419           | 0.0111     | -1.023    | 0.1818  | 0.0127 | 1.0841  | 0.9491  |         |

The theoretical transmission coefficient of the second model is much lower for both regular and random wave. The difference in performance was noted to be between 10.7 %-14.3 %.

Tables 8 and 9 on the next page summarize the experimental results for both non-porous and porous models.

Table 8: Experimental results for non-porous model ( $K_t$  1) at water depth 0.65 m

|        | Wave Gauge |            |            |            |            | $K_t$ 1 |         |
|--------|------------|------------|------------|------------|------------|---------|---------|
|        | A          | B          | C          | D          | E          |         |         |
|        | $H_s$ (mm) |         |         |
| Test1  | 161.415    | 154.918    | 127.229    | 127.695    | 127.706    | 0.7911  | Regular |
| Test2  | 164.96     | 158.052    | 150.163    | 123.253    | 148.117    | 0.7472  |         |
| Test3  | 155.453    | 198.432    | 153.339    | 166.444    | 167.916    | 1.0707  |         |
| Test4  | 180.947    | 156.874    | 122.242    | 136.44     | 130.079    | 0.7540  |         |
| Test 5 | 177.074    | 164.351    | 155.446    | 124.914    | 149.642    | 0.7054  |         |
| Test6  | 165.094    | 217.662    | 163.269    | 180.325    | 176.575    | 1.0923  |         |
| Test7  | 189.672    | 170.947    | 149.61     | 153.306    | 143.393    | 0.8083  |         |
| Test8  | 204.617    | 184.753    | 161.681    | 134.138    | 165.087    | 0.6556  |         |
| Test9  | 194.004    | 272.34     | 188.785    | 213.801    | 186.079    | 1.1020  |         |
| Test10 | 107.0515   | 121.698    | 103.496    | 98.55      | 95.827     | 0.9206  | Random  |
| Test11 | 94.1085    | 101.637    | 89.366     | 80.846     | 84.2525    | 0.8591  |         |
| Test12 | 81.4475    | 84.5605    | 76.6135    | 68.5325    | 72.012     | 0.8414  |         |

Table 9: Experimental results for porous model ( $K_t$  2) at water depth 0.65 m

|        | Wave Gauge |            |            |            |            | $K_t$ 2 |         |
|--------|------------|------------|------------|------------|------------|---------|---------|
|        | A          | B          | C          | D          | E          |         |         |
|        | $H_s$ (mm) |         |         |
| Test1  | 156.169    | 155.635    | 163.813    | 125.847    | 130.512    | 0.8058  | Regular |
| Test2  | 169.696    | 165.278    | 152.047    | 145.354    | 128.063    | 0.8566  |         |
| Test3  | 159.911    | 165.528    | 195.76     | 162.203    | 166.75     | 1.0143  |         |
| Test4  | 174.916    | 177.376    | 178.052    | 150.885    | 157.926    | 0.8626  |         |
| Test 5 | 187.728    | 191.918    | 170.128    | 161.759    | 143.976    | 0.8617  |         |
| Test6  | 182.261    | 191.858    | 221.752    | 184.037    | 180.804    | 1.0097  |         |
| Test7  | 187.286    | 198.892    | 196.014    | 166.136    | 165.854    | 0.8871  |         |
| Test8  | 213.562    | 214.854    | 204.688    | 181.343    | 151.545    | 0.8491  |         |
| Test9  | 197.658    | 197.706    | 249.721    | 192.556    | 202.019    | 0.9742  |         |
| Test10 | 109.6255   | 104.2135   | 117.734    | 96.472     | 91.283     | 0.8800  | Random  |
| Test11 | 93.233     | 91.0395    | 97.945     | 81.5405    | 76.639     | 0.8746  |         |
| Test12 | 77.9165    | 77.9185    | 80.4285    | 67.85      | 62.539     | 0.8708  |         |

The following Figure 17 and Figure 18 describe  $K_t$  as a function of  $B/L$ , given  $R_c/H_i$  for regular and random wave conditions respectively at water depth 0.65 m. 'T' denotes theoretical values whereas 'E' denotes experimental results.

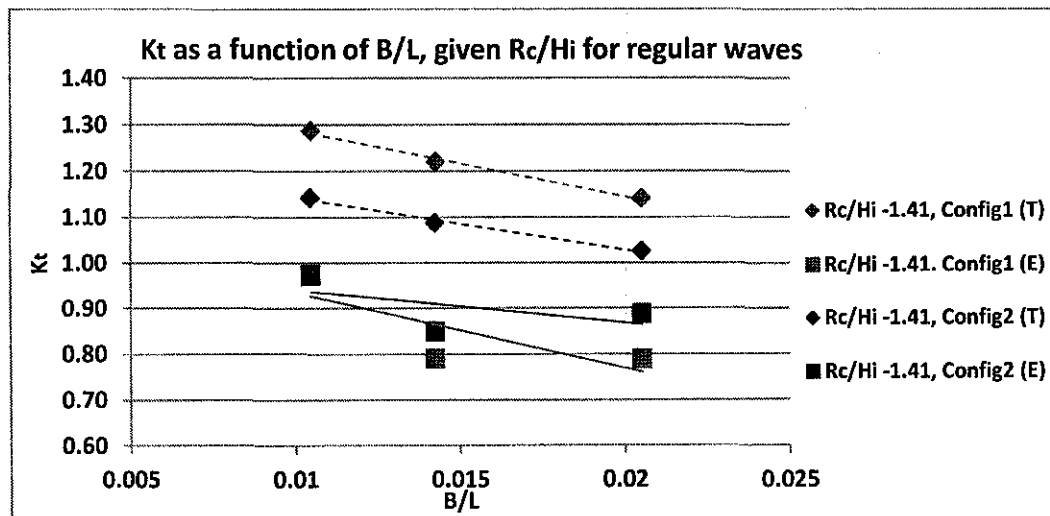
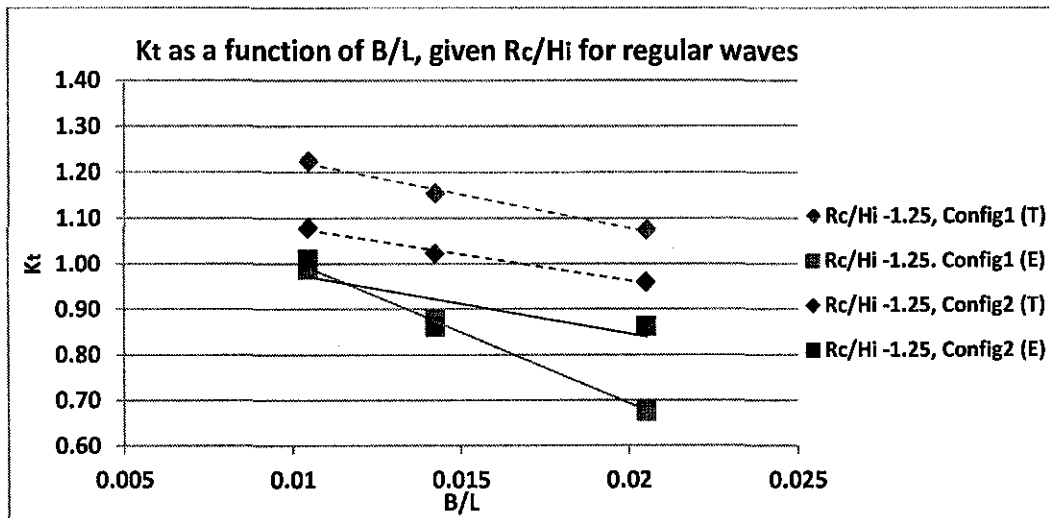
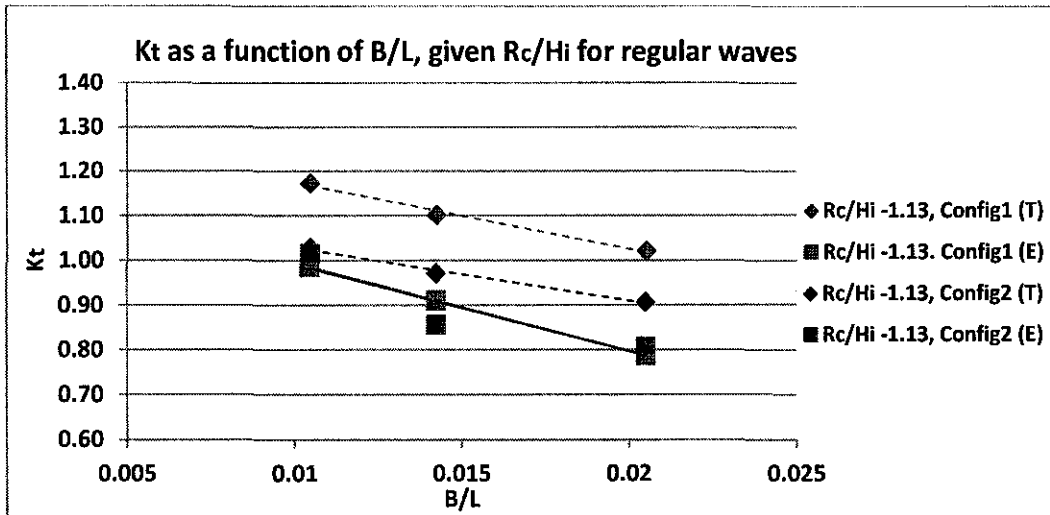


Figure 17:  $K_t$  as a function of  $B/L$ , given  $R_c/H_i$  for regular wave conditions  
( $d=0.65$  m)

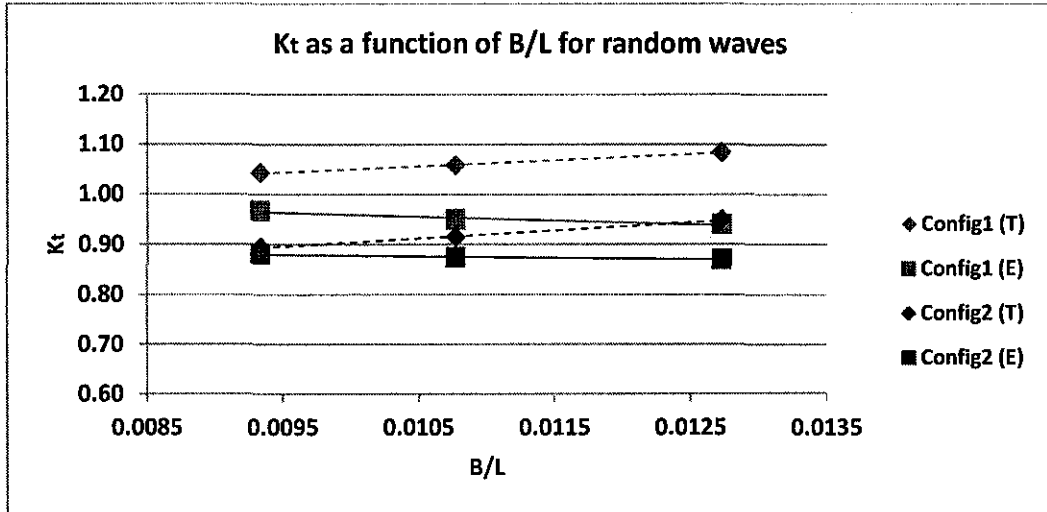


Figure 18:  $K_t$  as a function of  $B/L$ , given  $R_c/H_i$  for random waves at ( $d=0.65$  m)

The lowest transmission coefficient observed experimentally for the non-porous configuration is 0.66, which translate to a maximum wave reduction of 34 %. As for the porous configuration, the lowest transmission coefficient observed is 0.81.

Unlike previous runs, for both random and regular waves, the plots show a consistent range and trend of data, except for the non-porous mode. Hence at this water depth, it is observed that the performances of both sets are very comparable. A lower transmission coefficient is mostly achieved as  $B/L$  increases.

Figure 19 below describes  $K_t$  as a function of  $R_c/H_i$ , given  $B/L$  for regular wave conditions at water depth 0.65 m.

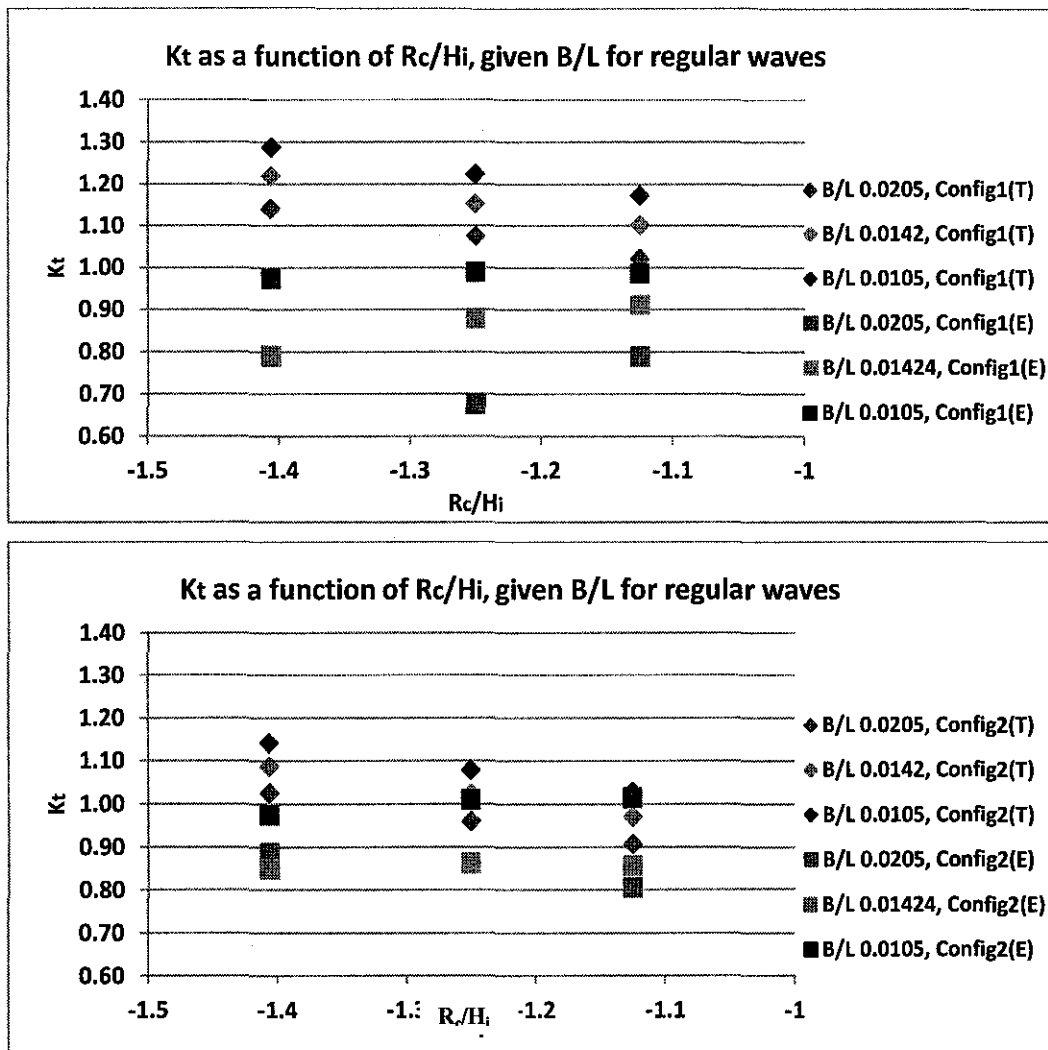


Figure 19:  $K_t$  as a function of  $R_c/H_i$ , given  $B/L$  for regular wave conditions ( $d=0.65$  m)

Figure 20 on the following page describes the relationship of  $K_t$  and  $R_c/H_i$ , given  $B/L$  for regular wave conditions at water depth 0.65 m.

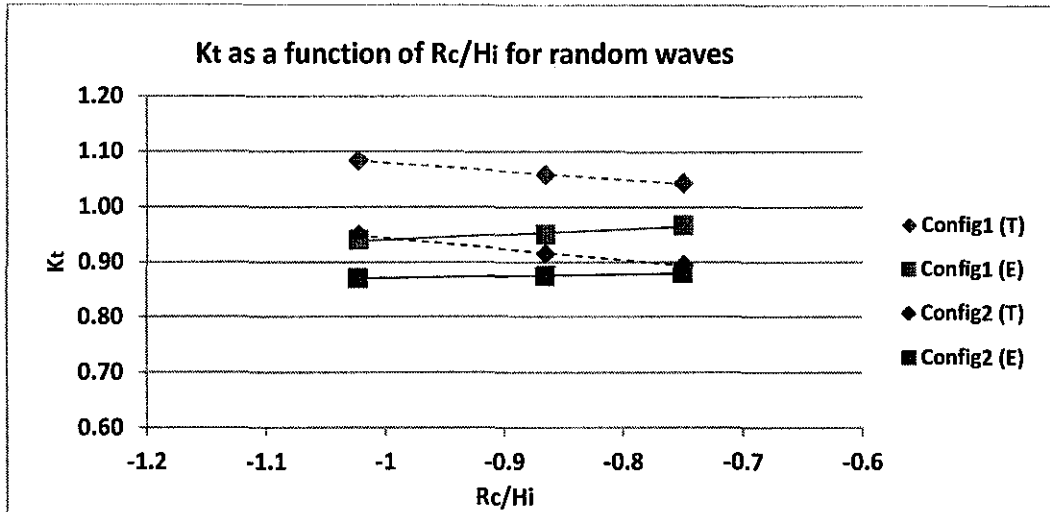


Figure 20:  $K_t$  as a function of  $R_c/H_i$  given  $B/L$  for random wave conditions ( $d=0.65$  m)

It is observed that a slight inverse coherence exist between the theoretical and experimental  $K_t$  for the both sets. As a rule of thumb, for the both sets of breakwater, given a constant  $R_c/H_i$ , the higher the  $B/L$ , the lower the  $K_t$ .

Figure 21 and Figure 22 depict the comparison of  $K_t$  for both regular and random wave conditions at water depth 0.65 m.

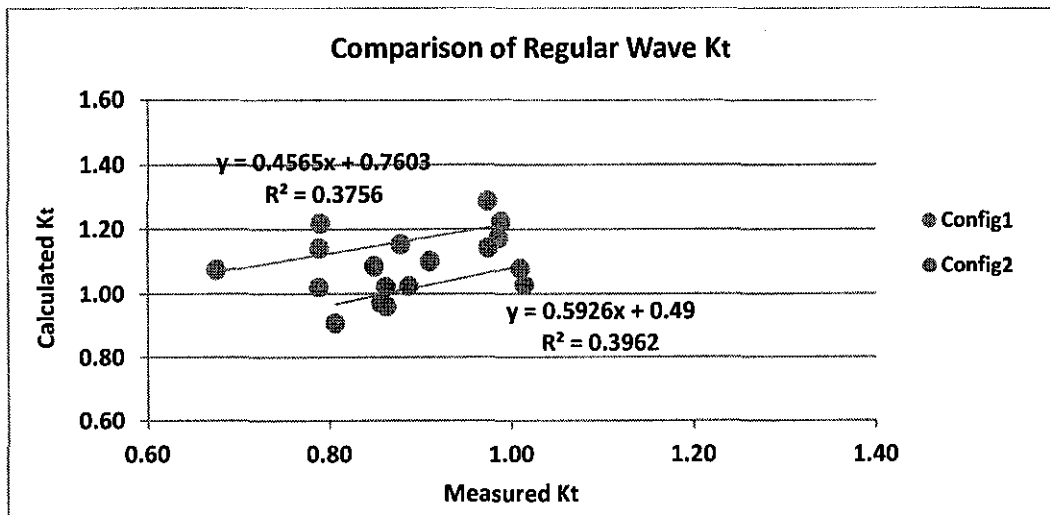


Figure 21: Comparison of calculated and measured  $K_t$  for regular wave conditions ( $d=0.65$  m)

The index of fit value ( $R^2$ ) was computed to be 0.38 and 0.396 for the non-porous and porous configuration respectively. This means that 38 % of variability in  $K_t$  of the non-porous set can be explained by Eq3 and its governing parameters. Likewise for the other set.

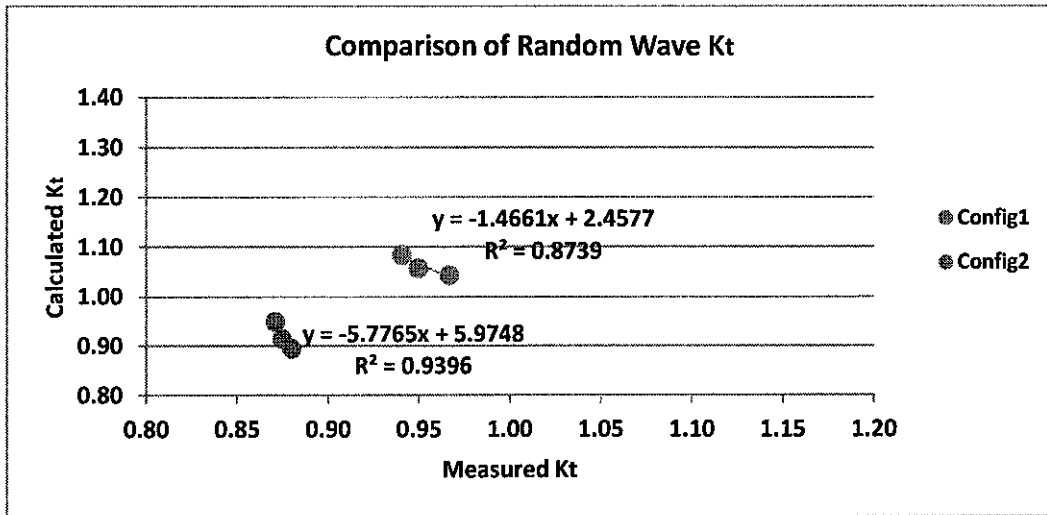


Figure 22: Comparison of calculated and measured  $K_t$  for random wave conditions ( $d=0.65$  m)

As for random waves, the index of fit value ( $R^2$ ) was computed to be 0.87 and 0.94 for the non-porous and porous configuration respectively.

### 4.3 Results for 0.60m water depth

Table 10 summarizes the wave parameters used as well as the theoretical transmission coefficient values for Non Porous ( $K_t1$ ) and Porous ( $K_t2$ ) Models.

Table 10: Summary of wave parameters and their corresponding transmission coefficient at water depth of 0.60 m

| Test | Wave Height (m) | Wave Period (s) | $H_i/gT^2$ | $R_c/H_i$ | $B/H_i$ | $B/L$  | $K_{t1}$ | $K_{t2}$ |         |
|------|-----------------|-----------------|------------|-----------|---------|--------|----------|----------|---------|
| 1    | 0.2             | 1.118           | 0.0163     | -0.875    | 0.2     | 0.0205 | 0.921    | 0.807    | Regular |
| 2    | 0.2             | 1.342           | 0.0113     | -0.875    | 0.2     | 0.0142 | 1.001    | 0.871    |         |
| 3    | 0.2             | 1.565           | 0.0083     | -0.875    | 0.2     | 0.0105 | 1.073    | 0.928    |         |
| 4    | 0.18            | 1.118           | 0.0147     | -0.972    | 0.222   | 0.0205 | 0.964    | 0.849    |         |
| 5    | 0.18            | 1.342           | 0.0109     | -0.972    | 0.222   | 0.0142 | 1.043    | 0.912    |         |
| 6    | 0.18            | 1.565           | 0.0749     | -0.972    | 0.222   | 0.0105 | 1.113    | 0.968    |         |
| 7    | 0.16            | 1.118           | 0.0131     | -1.094    | 0.25    | 0.0205 | 1.016    | 0.900    |         |
| 8    | 0.16            | 1.342           | 0.0091     | -1.094    | 0.25    | 0.0142 | 1.093    | 0.962    |         |
| 9    | 0.16            | 1.565           | 0.0067     | -1.094    | 0.25    | 0.0105 | 1.162    | 1.017    |         |
| 10   | 0.3             | 1.657           | 0.0111     | -0.583    | 0.1333  | 0.0093 | 0.9765   | 0.828    | Random  |
| 11   | 0.26            | 1.543           | 0.0111     | -0.673    | 0.1538  | 0.0108 | 0.9801   | 0.838    |         |
| 12   | 0.22            | 1.419           | 0.0111     | -0.795    | 0.1818  | 0.0127 | 0.9932   | 0.859    |         |

As speculated, the theoretical transmission coefficient of the second model is lower than the first model for both regular and random wave. The difference in performance was noted to be between 11.9 %-15.9 %.

Tables 11 and 12 summarize the experimental results for both non-porous and porous models.

Table 11: Experimental results for non-porous model ( $K_t$  1) at water depth 0.60 m

|        | Wave Gauge |            |            |            |            | $K_t$ 1 |         |
|--------|------------|------------|------------|------------|------------|---------|---------|
|        | A          | B          | C          | D          | E          |         |         |
|        | $H_s$ (mm) |         |         |
| Test1  | 161.415    | 154.918    | 127.229    | 127.695    | 127.706    | 0.7882  | Regular |
| Test2  | 164.96     | 158.052    | 150.163    | 123.253    | 148.117    | 0.9103  |         |
| Test3  | 155.453    | 198.432    | 153.339    | 166.444    | 167.916    | 0.9864  |         |
| Test4  | 180.947    | 156.874    | 122.242    | 136.44     | 130.079    | 0.6756  |         |
| Test 5 | 177.074    | 164.351    | 155.446    | 124.914    | 149.642    | 0.8779  |         |
| Test6  | 165.094    | 217.662    | 163.269    | 180.325    | 176.575    | 0.9889  |         |
| Test7  | 189.672    | 170.947    | 149.61     | 153.306    | 143.393    | 0.7888  |         |
| Test8  | 204.617    | 184.753    | 161.681    | 134.138    | 165.087    | 0.7902  |         |
| Test9  | 194.004    | 272.34     | 188.785    | 213.801    | 186.079    | 0.9731  |         |
| Test10 | 107.0515   | 121.698    | 103.496    | 98.55      | 95.827     | 0.9668  | Random  |
| Test11 | 94.1085    | 101.637    | 89.366     | 80.846     | 84.2525    | 0.9496  |         |
| Test12 | 81.4475    | 84.5605    | 76.6135    | 68.5325    | 72.012     | 0.9406  |         |

Table 12: Experimental results for non-porous model ( $K_t$  2) at water depth 0.60 m

|        | Wave Gauge |            |            |            |            | $K_t$ 2 |         |
|--------|------------|------------|------------|------------|------------|---------|---------|
|        | A          | B          | C          | D          | E          |         |         |
|        | $H_s$ (mm) |         |         |
| Test1  | 157.641    | 159.392    | 129.844    | 119.294    | 120.831    | 0.7665  | Regular |
| Test2  | 151.469    | 131.377    | 106.832    | 113.923    | 127.19     | 0.8397  |         |
| Test3  | 161.914    | 186.841    | 149.635    | 146.953    | 159.708    | 0.9864  |         |
| Test4  | 173.289    | 185.108    | 145.149    | 131.806    | 137.845    | 0.7955  |         |
| Test 5 | 174.146    | 145.71     | 113.629    | 114.169    | 125.087    | 0.7183  |         |
| Test6  | 182.606    | 205.189    | 163.595    | 157.132    | 162.871    | 0.8919  |         |
| Test7  | 187.773    | 209.284    | 147.198    | 109.639    | 128.126    | 0.6823  |         |
| Test8  | 199.437    | 174.305    | 130.064    | 131.761    | 129.555    | 0.6496  |         |
| Test9  | 194.117    | 200.627    | 162.077    | 156.501    | 168.883    | 0.8700  |         |
| Test10 | 107.0655   | 116.922    | 92.523     | 83.34      | 89.6555    | 0.8374  | Random  |
| Test11 | 92.433     | 97.4825    | 78.8795    | 70.4405    | 78.893     | 0.8535  |         |
| Test12 | 78.9215    | 79.754     | 65.269     | 57.465     | 67.7675    | 0.8587  |         |

Figure 23 and Figure 24 on the following pages describes  $K_t$  as a function of  $B/L$ , given  $R_c/H_i$  for regular and random wave conditions respectively at water depth 0.70 m. 'T' denotes theoretical values whereas 'E' denotes experimental results.

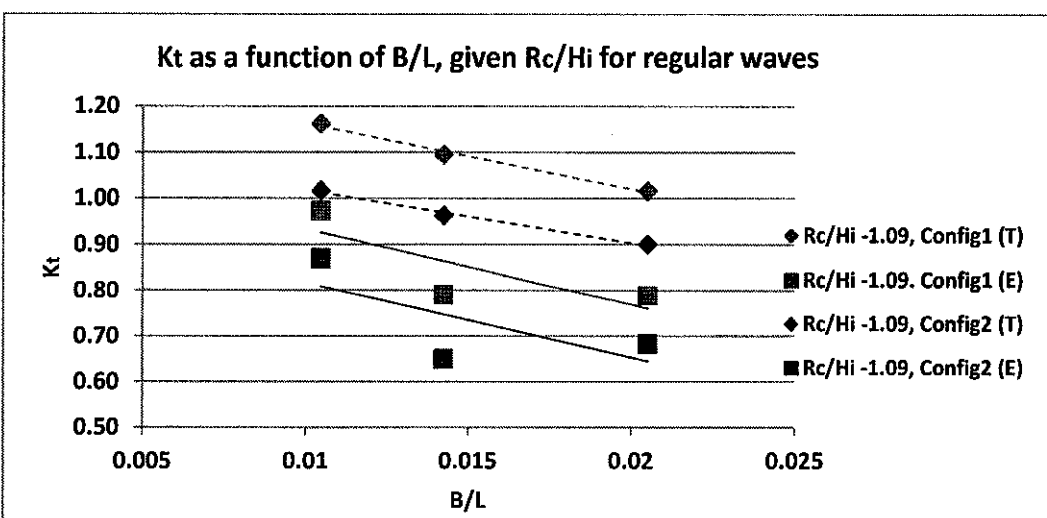
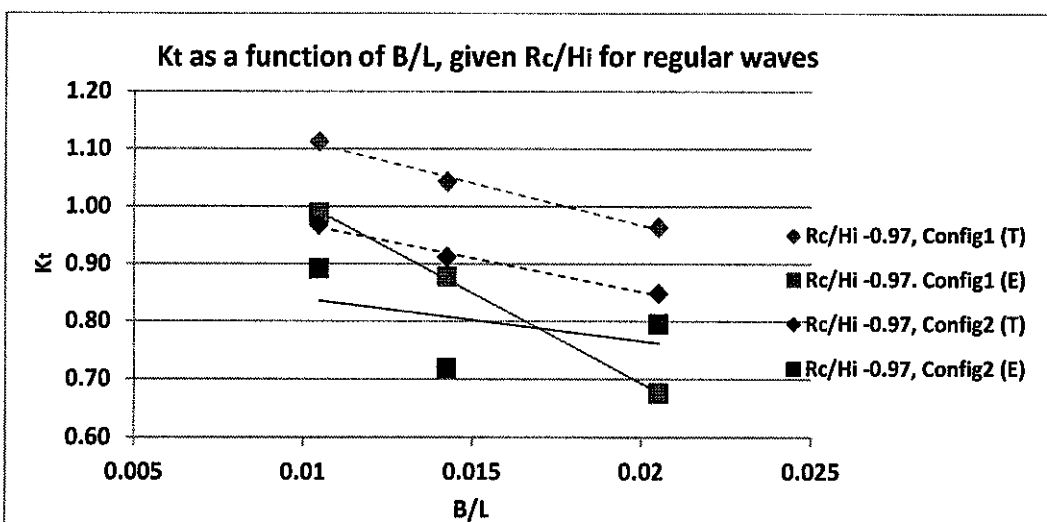
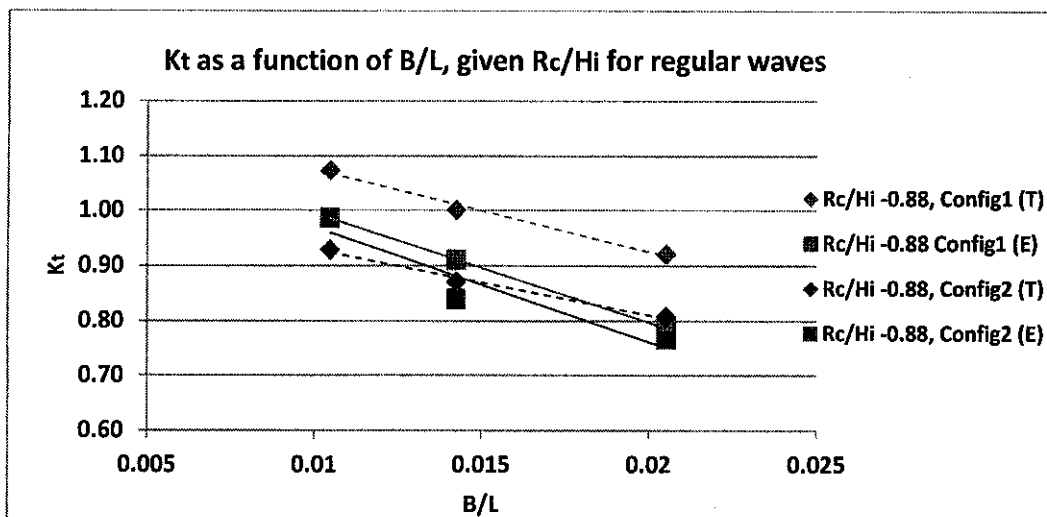


Figure 23:  $K_t$  as a function of  $B/L$ , given  $R_c/H_i$  for regular wave conditions  
( $d=0.60$  m)

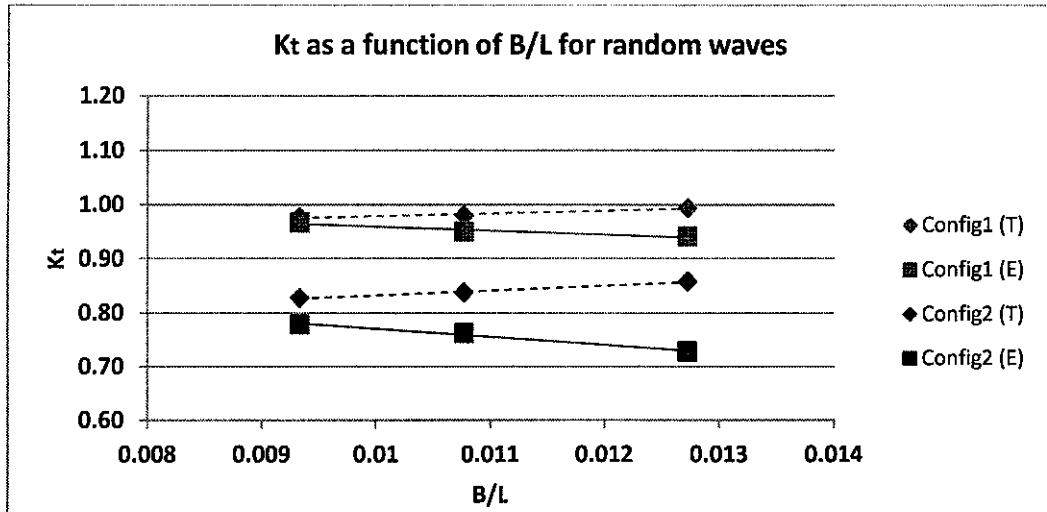


Figure 24:  $K_t$  as a function of  $B/L$ , given  $R_c/H_i$  for random wave conditions  
( $d=0.60$  m)

The lowest transmission coefficient observed experimentally for the non-porous configuration is 0.68, which translate to a maximum wave reduction of 32 %. As for the porous configuration, the lowest transmission coefficient observed is 0.65.

It is observed that a slight inverse coherence exist between the theoretical and experimental  $K_t$  for random wave conditions. As a rule of thumb, for the both sets of breakwater, given a constant  $R_c/H_i$ , the higher the  $B/L$ , the lower the  $K_t$ .

Figure 25 below describes  $K_t$  as a function of  $R_c/H_i$ , given  $B/L$  for regular wave conditions at water depth 0.60 m.

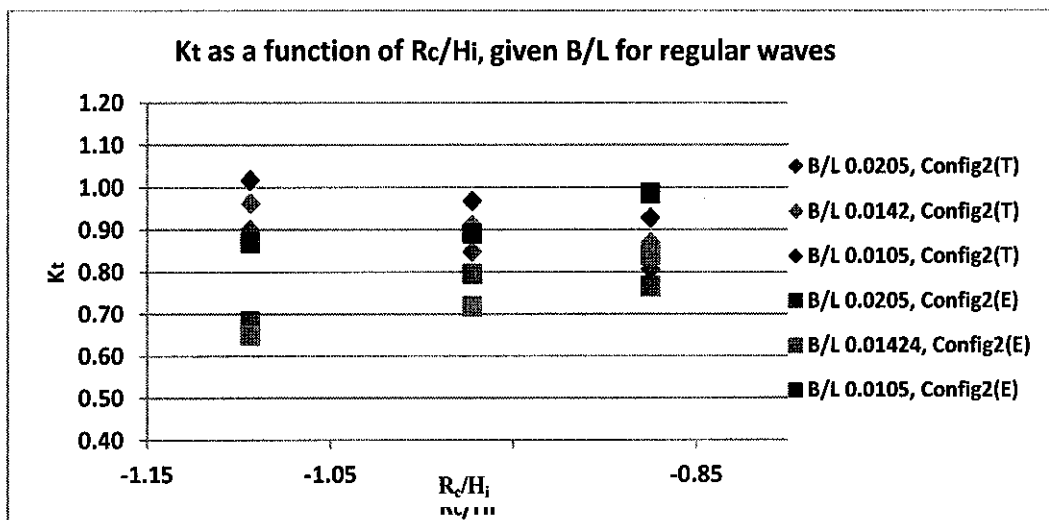
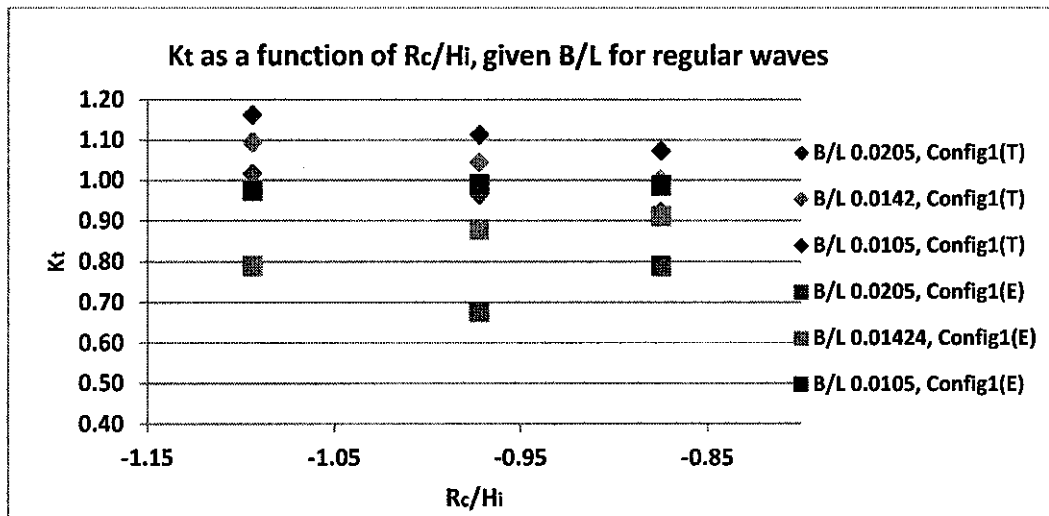


Figure 25:  $K_t$  as a function of  $R_c/H_i$  given  $B/L$  for regular wave conditions

( $d=0.60$  m)

Figure 26 on the following page describes the relationship of  $K_t$  and  $R_c/H_i$ , given  $B/L$  for regular wave conditions at water depth 0.60 m.

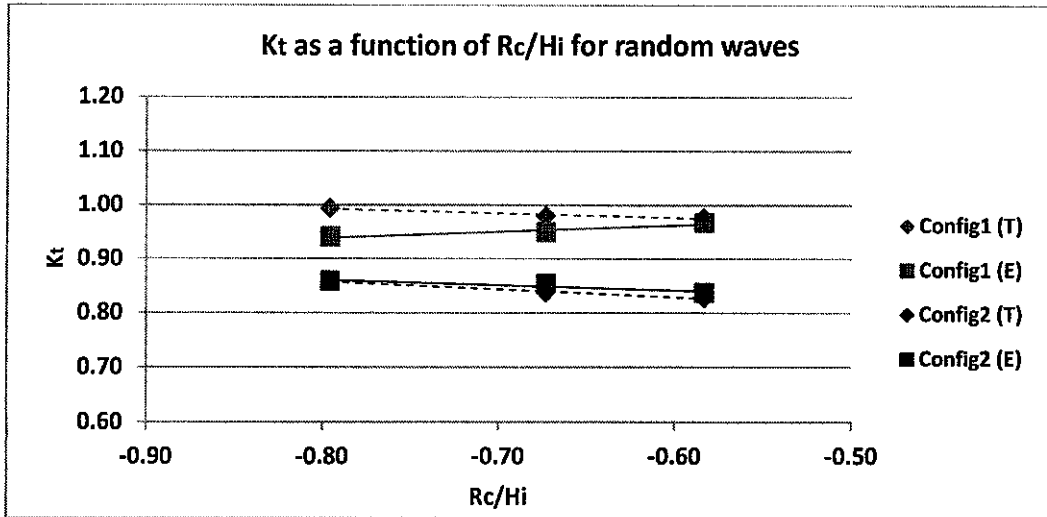


Figure 26:  $K_t$  as a function of  $R_c/H_i$  given  $B/L$  for random wave conditions ( $d=0.60$  m)

It is observed that a slight inverse coherence exist between the theoretical and experimental  $K_t$  for the both sets. Nevertheless, for the both sets of breakwaters, given a constant  $R_c/H_i$ ; the higher the  $B/L$ , the lower the  $K_t$ .

Figure 27 and Figure 28 depict the comparison of  $K_t$  for both regular and random wave conditions at water depth 0.60 m.

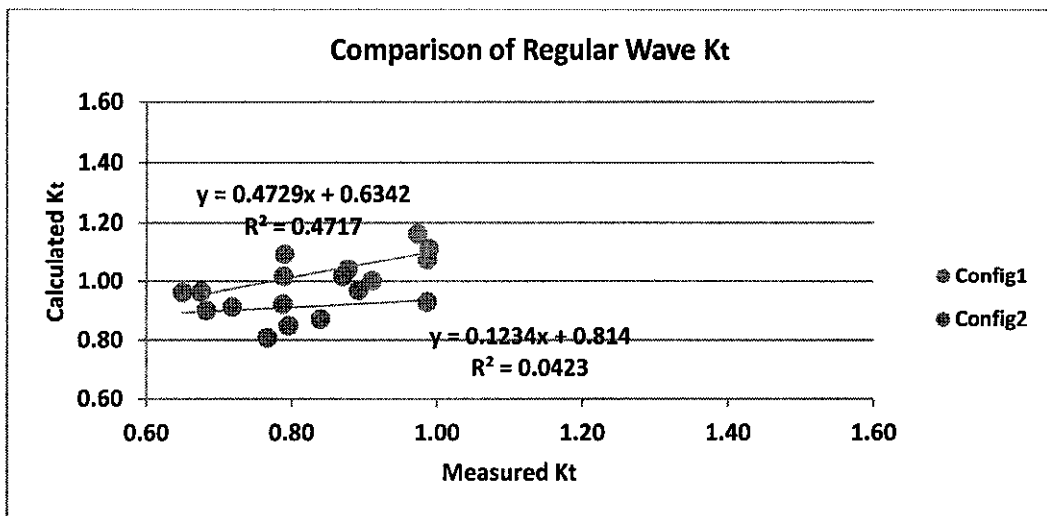


Figure 27: Comparison of calculated and measured  $K_t$  for regular wave conditions ( $d=0.60$  m)

The index of fit value ( $R^2$ ) was computed to be 0.47 and 0.04 for the non-porous and porous configuration respectively. This means that 47% of variability in  $K_t$

of the non-porous set can be explained by Eq. 3 and its governing parameters. Likewise for the other set. As for random waves, the index of fit value ( $R^2$ ) was computed to be 0.999 and 0.775 for the non-porous and porous configuration respectively, as shown below.

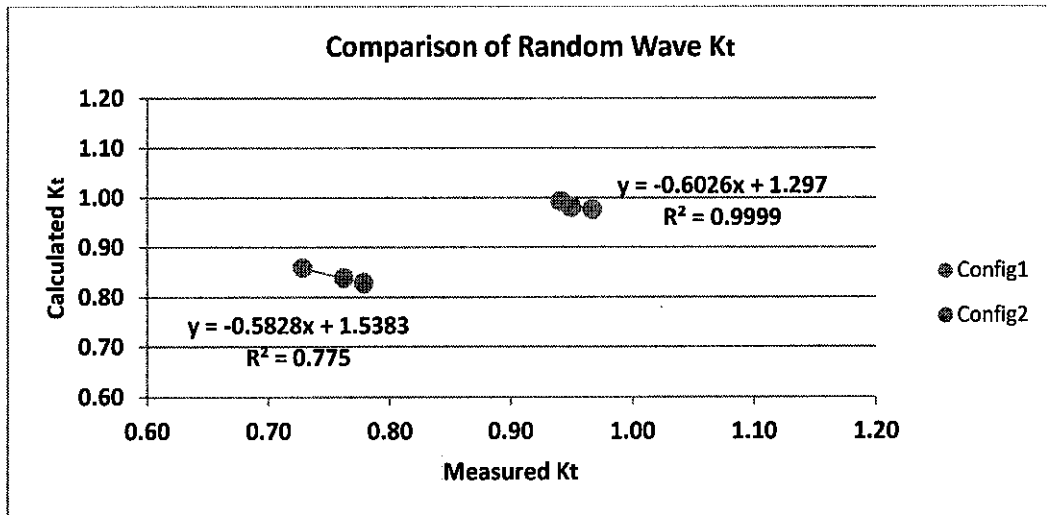


Figure 28: Comparison of calculated and measured  $K_t$  for random wave conditions ( $d=0.60$  m)

## CHAPTER 5

### CONCLUSION AND RECOMMENDATIONS

#### 5.1 Relevancy to the Objectives

Quantification of wave attenuation by an innovative submerged breakwater has been presented. The influence of water depth, incident wave height and period and structure porosity on wave transmission were investigated.

M-Sub has performed based on its wave attenuation objective, which is to reduce wave height behind the breakwater. Having the lowest transmission coefficients between a range of 0.68 and 0.81 for the tested water implies suitable wave conditions can be achieved at site in real application. Given the right modifications, the model could withstand moderate and low wave energy climate as intended.

Experimental results have yielded the following summarized conclusion:

- 1) The methodology d'Angremond provided realistic values of  $K_T$  within the range of tested parameters;
- 2) It was clear that the models were able to reduce the transmitted waves;
- 3) Analysing the relationship between transmission coefficient and relative structure length ( $B/L$ ), it was found that for same relative water depth ( $R_c/H_i$ ), the breakwater can further reduce the incident wave height as  $B/L$  increases. Take for instance, the porous configuration at 0.6 m water depth.

Given a wave height of 0.16 m and B/L of 0.0105, wave height reduction of the structure was 23%. However, when B/L was increased to 0.0205, its wave height reduction increased to 32%;

- 4) As the relative water depth increased, the reduction of wave height also intensified due to smaller incident wave heights;
- 5) Reduction of wave height was the most at the water depth of 0.60 m;
- 6) For water depth of 0.60 m, reduction of wave height were almost similar for tests involving the both sets of breakwater; and
- 7) Configuration 1 worked best for wave height of 0.18 m and wave period of 1.12 s. Whereas for configuration 2, the lowest  $K_t$  was recorded at wave height of 0.16 m.

## **5.2 Future Work and Recommendations**

Some recommendations should be performed to increase the accuracy of the physical model study and to investigate the performance of M-Sub. The recommendations are;

- 1) Potential modification on the design of the breakwater.  
The ability to interlock would be a plus point for the design to improve on the stability and performance of the structure under similar or greater wave conditions. A modification on the unit size might be performed as the current design has a limiting width in relation of longer wave lengths.
- 2) Further studies on different breakwater configuration.  
Different configurations of the breakwater can be studied to further enhance the stability and wave attenuating abilities of the breakwater. The crux of the design, which is the ability to dissipate wave energy through enhanced turbulences and vortices, should remain the focus of future designs
- 3) Additional testing on variations of wave characteristics.  
With more data to work on, one could obtain a better understanding of the relationship between the wave characteristics and the structure dimensions associated in the transmission (possible reflection and other non-pure transmission abilities) properties. With sufficient resources, numerical modeling can be done for further detailed studies.

## REFERENCES

- Ahrens, J.P. And Fulford, e.t., (1988). Wave energy dissipation by reef breakwaters. *Oceans '88, Marine Technology Society*, Washington, D.C., 1244–1249
- Artificial Reefs Org (n.d) Breakwater Wave Attenuation : Breakwater Geometry. Retrieved July 2011, from [www.artificialreefs.org](http://www.artificialreefs.org): <http://www.artificialreefs.org/ScientificReports/Wave%20reduction.htm>
- Baine, M. (2001). Artificial Reefs: A Review of their design, application, management and performance. *Ocean and Coastal Management*, 241-259
- Beck, M.W., Heck, K.L.J., Able, K.W., Childers, D.L., Eggleston, D.B., et al. (2001). The identification, conservation, and management of estuarine and marine nurseries for fish and invertebrates. *Bioscience* 51: 633–641
- Bohnsack J.A, Harper D.E, McClellan D.B and Hulsbeck M (1994). Effects of Reef Size on Colonisation and Assemblage Structure of Fishes at Artificial Reefs off Southeastern Florida, USA. *Bulletin of Marine Science*, 55: 796-823.
- Bortone S.A, Samoilyls M.A , Francour, P. (2000). Fish and Macro-Invertebrate Evaluation Methods. In *W.Seaman Jr (Ed.), Artificial Reef Evaluation with Application to Natural Marine Habitats*, CRC Press, Washington DC,127-164
- Church, J.W. (2007). Understanding Global Sea Levels: Past, Present and Future. Retrieved October, 2011 from [http://nora.nerc.ac.uk/5379/1/Church\\_et\\_al\\_-\\_Understanding\\_Global\\_Sea\\_Levels.pdf](http://nora.nerc.ac.uk/5379/1/Church_et_al_-_Understanding_Global_Sea_Levels.pdf)
- Coen, L. D., Luckenbach, M.W., Breitburg, D.L. (1999). The role of oyster reefs as essential fish habitat: a review of current knowledge and some new perspectives. *American Fisheries Society Symposium* 22: 438–454.
- Cummings S.L (1994) Colonisation of a NearShore Artificial Reef at Boca Raton (Palm Beach County), Florida. *Bulletin of Marine Science* 55: 1193-1215.

d'Angremond, K., Van der Meer, J.W., and de Jong, R.J. (1996). Wave Transmission At Low-Crested Structures, *25th Int. Conf. on Coastal Eng.*, Orlando, Florida.

Department of Irrigation and Drainage Malaysia. (n.d.). The Official Website for the Department of Irrigation and Drainage Malaysia. Retrieved June 22, 2011, from [www.water.gov.my](http://www.water.gov.my):

[http://www.water.gov.my/index.php?option=com\\_content&task=view&id=30&Itemid=184](http://www.water.gov.my/index.php?option=com_content&task=view&id=30&Itemid=184)

Sidek, F. (2007). The Effects of Porosity of Submerged Breakwater Structures on Non-Breaking Wave Transformation. *Malaysian Journal of Civil Engineering*, 17-25.

Golani,D and Diamant,A (1999). Fish Colonisation of an Artificial Reef in the Gulf of Elat, Northern Red Sea. *Environmental Biology of Fishes*, 54:275-28

Grove, R.S and Sonu, C.J (1983). Review of Japanese Fishing Reef Technology. *Fisheries Research* 83, Southern California Edison Company, Rosemead, California

Gunter, G. (1967). Some Relationships of Estuaries to the Fisheries of the Gulf of Mexico, *American Association for the Advancement of Science*. pp. 621–638.

Heck, K.L., Hays, G., Orth, R.J. (2003). Critical evaluation of the nursery role hypothesis for seagrass meadows. *Marine Ecology Progress Series* 253: 123–136.

J.B.Herbich. (2000). *Handbook of Coastal Engineering*. McGraw-Hill.

Jara,F. and Cespedes R. (1994) An Experimental Evaluation of Habitat Enhancement on Homogeneous Marine Bottoms in Southern Chile. *Bulletin of Marine Science*, 55(2-3); 295-307.

Lindquist, D.G. and Pietrafesa, L.J. (1989) Current Vortices and Fish Aggregations: The Current Field and Associated Fishes around a Tugboat Wreck in Onslow Bay, North Carolina. *Bulletin of Marine Science*, 44(2), 533-54

Moreno, C.A and Jara H.F (1984) Ecological Studies of fish fauna associated with *Macrocystis pyrifera* belts in the south of Fuegian Islands, Chile. *Mar.Ecol. Prog. Ser* 15:99-107

Palmer, G.N and Christian, C.D (1998) Design and construction of rubble mound breakwaters, *IPENZ Transactions*, Vol.25. Bo. 1/CE, 1998

Pilarczyk, K. W. (2003). Design of low crested(submerged) structures: An Overview. 6th International Conference on Coastal and Port Engineering in Developing Countries. Colombo, Sri Lanka.

Proceedings of Workshop on Artificial Reefs for the Enhancement of Fishery Resources. SEAFDEC/FRA Joint Program Regarding Artificial Reefs for the Enhancement of Fishery Resources, August 2009, Putrajaya, Malaysia.

Ranasinghe, R., Hacking, N. and Evan, P. (2001). Multi-functional artificial surf breaks: A Review, *Report No. CNR 2001.015, NSW Dept. of Land and Water Conservation, Parramatta, Australia*

Reef Check . (n.d.). Retrieved June 19, 2011, from [www.reefcheck.org.my](http://www.reefcheck.org.my):  
<http://www.reefcheck.org/PDFs/reports/Malaysia%202010%20Survey%20Report.pdf>

Swann, L. (2008). The Use of Living Shorelines to Mitigate the Effects of Storm Events on Dauphin Island, Alabama, USA. American Fisheries Society Symposium. 64. American Fisheries Society.

Uda, T. (1998) Function and design methods of artificial reef, Ministry of Construction, Japan

US Army Corps of Engineers. (1984). Shore Protection Manual, Coastal Engineering Research Center, Fort Belvoir, Virginia.

US Army Corps of Engineers. (2009, July 16). Publication: Coastal Engineering Manual. Retrieved June 19, 2011, from Coastal and Hydraulics Laboratory - Engineer Research and Development Center:  
[http://140.194.76.129/publications/eng-manuals/em1110-2-1100/PartIII/Part-III-Chap\\_5entire.pdf](http://140.194.76.129/publications/eng-manuals/em1110-2-1100/PartIII/Part-III-Chap_5entire.pdf)

Van Der Meer (1995) Conceptual Design of Rubble Mound Breakwater. Retrieved July 2011, from :  
[http://www.vandermeerconsulting.nl/downloads/stability\\_b/1995\\_vandermeer\\_conceptualdesign.pdf](http://www.vandermeerconsulting.nl/downloads/stability_b/1995_vandermeer_conceptualdesign.pdf)

Welsh, J.P and Koerner R.M (1979) Innovative Uses of Synthetic Fabrics in Coastal Construction. *Coastal Structures '79, American Society of Civil Engineers, New York, NY*, 364-372

Wildasia Org (2005) Introduction: What is a coral reef? Retrieved August 2011 from [www.wildasia.org](http://www.wildasia.org) :  
[http://www.wildasia.org/main.cfm/support/Coral\\_Reef\\_Conservation](http://www.wildasia.org/main.cfm/support/Coral_Reef_Conservation)

## **APPENDIX A: WAVE CHARACTERISTICS OF EAST COAST**

Wave condition in Malaysia is influenced by the northeast monsoon and the southwest monsoon wind. Higher average wind waves of 1.0 to 1.5 m occur during the NE monsoon season from the months of November to March.

The corresponding average period is around 2.5 to 5.0 s. Higher wind waves of 2.5 to 3.0 m are more likely to occur in the middle of the NE monsoon period (December and January). It is to be noted that MMS data are largely derived to **avoid rough sea conditions.**

In the SW monsoon season from June to September, the average wind waves between 0.7 to 1.1 m in height with the corresponding period averaging around 2.0 to 4.0 s. The maximum height of wind wave during this period is around 2.0 m.

In the months in between the two monsoon periods ( April, May and October), the height of the wind waves are around 0.7 m and with the corresponding period of 2.0 to 4.0 s. The maximum height of wind wave in this period is around 2.0 m. This shows that the wind waves heights in Malaysian waters especially in the areas facing South China Sea has peak (northeast monsoon season) and valley (period in between the two monsoon seasons).

Similar behaviour occurs for the swell conditions in Malaysian waters. Swell of 1.5 to 2.0 m occur during the NE monsoon season. The corresponding period average around 4.0 to 5.0 s, with maximum swell of 2.5 to 3.0 m likely to occur in the middle of the NE monsoon period. In the SW monsoon season, swell averages between 1.0 to 1.5 m in height with the corresponding period averaging around 4.0 to 5.0 s occurring during this period. The maximum height of swell during this period is around 2.0 to 2.5 m. In the months in-between the two monsoon periods, the swell height is around 1.0 to 1.5 m and with the corresponding period of 4.0 to 5.0 s. The maximum height of swell in this period is around 2.0 to 2.5 m.

The directions of wave in Malaysia are influenced by the monsoon wind.

In the NE monsoon period, the predominant wave direction is from the east quadrant for locations in the east peninsular Malaysia, Sarawak and Sabah except for west peninsular Malaysia which is from the south quadrant. In the months of April to May, the wave direction gradually changes from east to southwest quadrant. In the southwest monsoon period, the wave direction is from the southwest quadrant for all location. In October, predominant wave direction is from the southwest quadrant.

The climatology of ocean waves and wind is based on the monthly summary of marine meteorological observations published by the Malaysian Meteorological Service (MMS), covering the period of 1985-2000. The wave and wind data collected are derived from marine surface observations reported by ships which participated in the World Meteorological Organization Voluntary Observation Ships Scheme, oilrigs and lighthouses.

#### References

- [1] MMS. Monthly summary of marine meteorological observations, Malaysian Meteorological Service, Malaysia (1985-2000)
- [2] E.P. Chiang, Z. A. Zainal, P.A. Aswatha Narayana, K.N. Seetharamu (2003) Potential of Renewable Wave and Offshore Wind Energy Sources in Malaysia

## APPENDIX B: MISCELLANEOUS

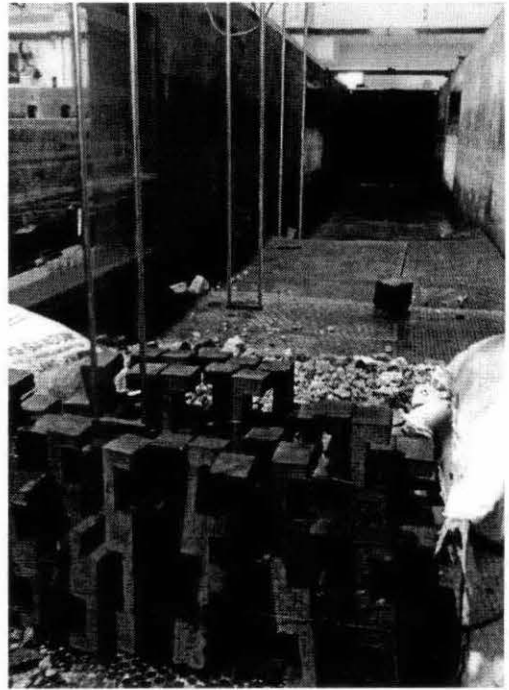


Figure A-1: (Left) Setting up of experimental tests  
breakwater set

(Right) The porous